First published online as a Review in Advance on January 2, 2008

Choreography of Cell Motility and Interaction Dynamics Imaged by Two-Photon Microscopy in Lymphoid Organs

Michael D. Cahalan[1,3] and Ian Parker[1,2]

[1]Department of Physiology and Biophysics, [2]Department of Neurobiology and Behavior, and [3]Center for Immunology, University of California, Irvine, California 92697; emails: mcahalan@uci.edu, iparker@uci.edu

Annu. Rev. Immunol. 2008. 26:585–626

The *Annual Review of Immunology* is online at immunol.annualreviews.org

This article's doi: 10.1146/annurev.immunol.24.021605.090620

0732-0582/08/0423-0585$20.00

Key Words

T cell, B cell, dendritic cell, chemokine, antigen, motility

Abstract

The immune system is the most diffuse cellular system in the body. Accordingly, long-range migration of cells and short-range communication by local chemical signaling and by cell-cell contacts are vital to the control of an immune response. Cellular homing and migration within lymphoid organs, antigen recognition, and cell signaling and activation are clearly vital during an immune response, but these events had not been directly observed in vivo until recently. Introduced to the field of immunology in 2002, two-photon microscopy is the method of choice for visualizing living cells deep within native tissue environments, and it is now revealing an elegant cellular choreography that underlies the adaptive immune response to antigen challenge. We review cellular dynamics and molecular factors that contribute to basal motility of lymphocytes in the lymph node and cellular interactions leading to antigen capture and recognition, T cell activation, B cell activation, cytolytic effector function, and antibody production.

INTRODUCTION

The immune system is designed for detection of foreign antigens that have never been encountered, for amplification of responses to previously encountered antigen, and for the delivery of coordinated effector responses ranging from mobilization of effector T cells, cytokine delivery, and antibody production. Each of these processes relies on cell-to-cell contact for initiation, followed by guided dispersal of effector cells and molecules to the appropriate location, while avoiding friendly fire that could result in autoimmune disease. Lymphocytes are potentially dangerous cells, and numerous cellular and molecular mechanisms avoid inappropriate triggering, dampen initial responses, and amplify responses to second and subsequent encounters with antigen, while at the same time optimizing sensitivity to minute quantities of antigen. Within the past five years, since publication of the first studies examining the motility of lymphocytes and thymocytes in native tissue environments (1–3), new imaging studies have appeared at an exponentially increasing rate. Two-photon microscopy has proved to be the method of choice for cellular immunoimaging, enabling visualization deep within intact organs and tissues while minimizing photodamage and bleaching. Efforts to map out the cellular choreography in vivo build upon a framework of in vitro studies of lymphocyte motility and response dynamics following contact with antigen-presenting cells (APCs).

In this review, we first discuss the technology of two-photon microscopy as applied to immunoimaging and then focus on its applications to live-cell imaging of immune cells in the lymph node under basal conditions and in response to antigenic challenge. Collectively, two-photon microscopy is revealing an elaborate and elegant choreography of cell motility, antigen capture, and cell-cell interactions in a variety of in vivo settings and holds great promise for understanding the dynamic response to infectious agents.

TWO-PHOTON IMAGING METHODOLOGY

Imaging the single-cell dynamics of the immune system within an intact environment requires the ability to look deep inside intact tissues and organisms with spatial and temporal resolution adequate to track cell morphology, motility, and signaling processes, all the while minimizing perturbation of the system under study. Optical microscopy employing fluorescence techniques is highly suited for this purpose, permitting both labeling of specific cells, organelles, or proteins and functional readout of physiological events (4). However, conventional (single-photon) techniques such as wide-field and confocal microscopy suffer severe disadvantages, principally because the short wavelengths required for fluorescence excitation are subject to strong scattering in biological tissue and exacerbate phototoxicity. Nonlinear microscopy differs fundamentally from conventional techniques in that the elementary process involves near simultaneous interactions of two (or more) photons, so that the signal varies as the square (or higher power) of incident light intensity, rather than linearly. This nonlinear relationship leads to qualitatively new imaging modalities, of which fluorescence excitation by two-photon absorption and second harmonic generation have proved most useful for immunoimaging.

The essence of two-photon microscopy is that a fluorophore is excited by the near-simultaneous absorption of energy from two photons, each of which contributes one half of the energy required to induce fluorescence. Because excitation then increases as the square of the incident light intensity, fluorescence is essentially confined to the focal spot formed by a microscope objective, thereby providing an inherent optical sectioning effect, analogous (though involving a completely different mechanism) to confocal microscopy. To achieve practicable fluorescence signals, the photon density in the focal spot must be incredibly high, yet not so high as to damage the specimen. This is achieved by using

femtosecond or picosecond pulsed lasers, which concentrate their output into brief bursts with enormous instantaneous power, yielding a two-photon advantage of $\sim 10^5$ as compared with a continuous beam of the same average power. The continuing improvement of ultrafast pulsed lasers has been a key factor driving the adoption of two-photon microscopy by immunologists.

In addition to its inherent optical sectioning effect, two-photon excitation has other major advantages for immunoimaging because the excitation wavelengths are roughly twice as long as would be used for conventional linear excitation by widefield or confocal microscopy. This use of long wavelength excitation is particularly advantageous for imaging deep into highly scattering biological tissues (5) because scattering decreases with increasing wavelength (6) and because absorption by hemoglobin and other proteins is minimized. Thus, the infrared wavelengths used for two-photon imaging enable a fivefold or deeper tissue penetration than does confocal imaging employing visible wavelengths (2, 7–9) and cause negligible photodamage or photobleaching. Long-term imaging is thereby facilitated because bleaching and damage processes (induced by nonlinear processes) are largely confined to those cells lying at the focal plane, whereas cells above and below experience only the innocuous infrared light. Nevertheless, the laser power must be kept below some sharp threshold value in order to maintain long-term viability of the preparation. Finally, the two-photon excitation spectra of most fluorophores are appreciably broader than for one-photon excitation (10), so a single excitation wavelength can be used efficiently to excite multiple probes simultaneously with distinct emission wavelengths. Moreover, the ease of tuning of the latest generations of femtosecond lasers facilitates selection of a wavelength that balances excitation of different fluorophores. In instances in which highly divergent excitation wavelengths are required, two independently tuned lasers may be used simultaneously (8).

In addition to multiphoton absorption, another nonlinear interaction that becomes prominent at very high light intensities is that of optical-harmonic generation, in which two (or more) photons are almost simultaneously scattered to generate a single photon with exactly twice (or higher multiples of) the incoming energy (11). Second harmonic generation is produced by spatially ordered molecules and has proved especially useful for imaging ordered structural proteins such as collagen fibers (12) and microtubules (13) by detecting emitted light through a bandpass filter of twice the wavelength of the excitation light without the need for fluorescent labeling.

Deep tissue imaging is currently limited by several factors, including the requirement for exponentially increasing excitation power at increasing depths to compensate for increasing scattering loss. Use of infrared-emitting dyes may be advantageous in reducing signal loss owing to scattering, and the advent of ever more powerful lasers extends the depth range but will be limited by thermal effects and excitation near the surface (5). Moreover, image quality (as well as brightness) degrades with transit through tissues with strongly varying refractive index but may be mitigated by correcting for wavefront distortions with deformable mirrors (14) or by applying depth-dependent deconvolution algorithms to acquired images (15). Imaging yet deeper into thick tissues and organs will necessitate mechanical techniques, such as penetration or removal of overlying tissue, use of needle-like gradient index lenses to extend the range of otherwise bulky objectives (13), and development of miniaturized two-photon endoscopes (16, 17).

Fluorescent Labels and Probes

The imaging techniques reviewed here rely primarily on the introduction of a fluorescent probe or label into cells or structures of interest, although useful information may also be gained from intrinsic signals such as autofluorescence and second harmonic generation.

Extrinsic labeling may be accomplished in vitro using isolated cells that are then adoptively transferred into a recipient animal by introducing fluorophores directly into the animal or organ being imaged (e.g., to stain vasculature) or by genetically engineering expression of fluorescent proteins.

The first in situ imaging studies of lymphocytes and dendritic cells (DCs) employed cell tracker fluorescent dyes, including CSFE (5,6-carboxyfluoresceine diacetate succinimidyl ester; green fluorescence) and CMTMR (chloromethylbenzoyl aminotetramethylrhodamine; red) for staining of adoptively transferred cells, and this method remains a mainstay. Such dyes have been used for many years by immunologists for flow cytometry and have the advantages of providing bright fluorescence signals while being relatively benign. Adoptive transfer of labeled cells typically results in <1% of cells being labeled in dense tissue populated by a vast excess of unlabeled cells. Although this is a huge advantage for tracking single cells and visualizing their morphological characteristics, it is obviously important that the unseen cells may exert significant effects on the labeled cells. The proportion of labeled cells can be adjusted to vary the density of labeled cells. Differently labeled cells can be coinjected and then distinguished by color. This approach has several advantages: It creates an internal control population for comparison; it allows labeling of a tissue landmark or compartment, such as the follicle, for orientation while imaging; and it allows comparison of cells by molecular perturbation with a drug treatment or a genetic deletion.

Dyes are available with a wide range of emission spectra separated sufficiently to permit independent visualization of at least three cell populations separately labeled with, for example, blue-, green-, and red-emitting dyes, by use of appropriate dichroic mirrors and bandpass filters before three photomultiplier detectors. Moreover, using dyes such as CFSE, one can track the number of times that lymphocytes divide in vitro or in vivo by taking advantage of the fact that the original dye content is split equally into the daughter cells each time the cell divides. Thus, comparison of relative fluorescence intensities among cells can be an indicator of how many times they have divided. However, this approach is complicated by the need to correct for variation in signal intensity with imaging depth into the tissue, and after a few cycles the remaining fluorescence becomes too faint to detect so that it is not possible to visualize labeled lymphocytes for more than one or two days after antigen stimulation or to follow them into peripheral sites of effector function. Significant disadvantages of in vitro dye labeling approaches arise because cells must first be extracted from their normal environment in the donor animal before adoptive transfer into the recipient host.

Expression of fluorescent proteins by target cells has been the other main method for visualizing target cells. The original fluorescent proteins derived from the Aequorea green fluorescent protein (GFP) suffered from low brightness and closely overlapping emission spectra. Subsequent developments, including the identification of a red fluorescent protein from the coral *Discosoma* and extensive mutagenesis work, have now made available a wide range of fluorescent proteins with peak emissions ranging from blue (475 nm) to red (610 nm), which have greatly improved properties in terms of brightness, lack of pH sensitivity, faster maturation, and lack of oligomerization (reviewed in 18, 19). The two-photon excitation maxima for fluorescent proteins generally lie at longer wavelengths (approximately 900 nm) (20) than for organic dyes (approximately 780 nm). Simultaneous imaging of both types of label with a single femtosecond laser thus requires selection of an intermediate wavelength that provides an optimal compromise, whereas application of a dual, independently tuned laser system may offer appreciable advantage. The fluorescence brightness obtained from a cell obviously depends on the level of protein expression and must be balanced against the

possibility of cellular disruption with overexpression systems, particularly when the fluorescent protein is tagged to some other protein of interest.

There are several advantages to using expressed fluorescent proteins over other extrinsic fluorophores: (*a*) The label is not diluted by successive cell divisions, allowing tracking of cell progeny after clonal expansion. Using a mouse with GFP under the control of a ubiquitous promoter such as β-actin or ubiquitin, T or B cells can be purified and adoptively transferred into recipients. For longer-term tracking, the recipient of choice would be one that has been tolerized by tissue-specific expression of GFP elsewhere, avoiding immune responses to GFP (21). (*b*) Fluorescent proteins can be expressed under the control of specific promoters to obtain selective expression of a particular cell type. For example, the CD11c promoter has been used to drive expression of YFP in DCs (22). The advantage of being able to visualize every cell of a particular cell type must be weighed against the potential difficulty of tracking individual cell behavior in densely populated tissue. An analogy may be made with Golgi staining of the nervous system, which reveals the morphological complexity of sparsely labeled individual neurons in the brain. (*c*) Specific proteins may be directly tagged with a fluorescent protein to visualize in real time their subcellular expression and/or relocalization, rather than merely expressing free cytosolic fluorescent protein as a cellular marker. (*d*) Transgenic expression of fluorescent proteins enables in situ labeling of cells, so that for many experiments the need for ex vivo manipulations is eliminated. (*e*) The percentage of a particular cell type that expresses a fluorescent protein can be adjusted by making mixed bone marrow chimeras (23, 24), thus facilitating tracking of individual cell behavior. (*f*) Immune cells can be selectively ablated by irradiation in a mouse that ubiquitously expresses fluorescent protein and then reconstituted from bone marrow of a nonfluorescent donor, allowing radiation-resistant stromal and vascular cells to be visualized (25).

Analyzing Cell Motility and Interactions

Multiphoton imaging yields 4-D (*x*, *y*, *z*, *t*) information of cell morphology and motility, but the very wealth of data (gigabytes) presents appreciable problems of visualization and analysis. The results are almost impossible to convey in static images on the printed page but are better appreciated as time-lapse movies, usually presented as maximum-intensity 2-D projections along the *z*-axis. Depth information is lost in this process (so it is impossible to discern whether cells touch or pass over one another), but it may be communicated by methods such as color-encoding the *z*-axis location of cells (26) or employing specialized 3-D visualization software.

The instant replay of time-lapse videos is, however, only a first step in immunoimaging, and deriving quantitative information by tracking cells is crucial (**Figure 1**). Quantitative tracking is most easily achieved by 2-D analysis after compression of image stacks, a procedure that circumvents errors that are due to the inherently lower *z*-axis resolution. 3-D tracking is essential in cases in which motility may be anisotropic in the *z*-axis. Cell tracks may be superimposed directly on the imaging field (**Figure 1*a***) or, if there are no reasons to suspect regional differences, by overlaying tracks from several cells after normalizing their starting coordinates to generate a flower plot (**Figure 1*b***). Various parameters (**Table 1**) can then be extracted from such tracking data to characterize cell motility and morphology (**Figure 1*c*,*d***). Instantaneous velocity is a simple and widely used parameter, but it is subject to errors. For example, jitter in measurements at brief time steps overestimates velocities and can give the appearance of motion in even stationary cells, whereas time steps longer than the persistence time for linear motion will tend to underestimate velocities.

Early imaging studies (2) suggested that T cell motility in the lymph node approximates a random walk, and several approaches have subsequently been adopted to characterize whether motility is indeed random or is directed (e.g., along chemokine gradients). For a random-walk process, the mean displacement from origin increases as a square root function with time. Analogous to the diffusion coefficient for Brownian motion, the slope of this relationship can be used to calculate a motility coefficient. This has generally been done by plotting displacement versus square root of time (**Figure 1*e***) (2), but a plot of displacement squared versus time is more appropriate when data are appreciably scattered. A

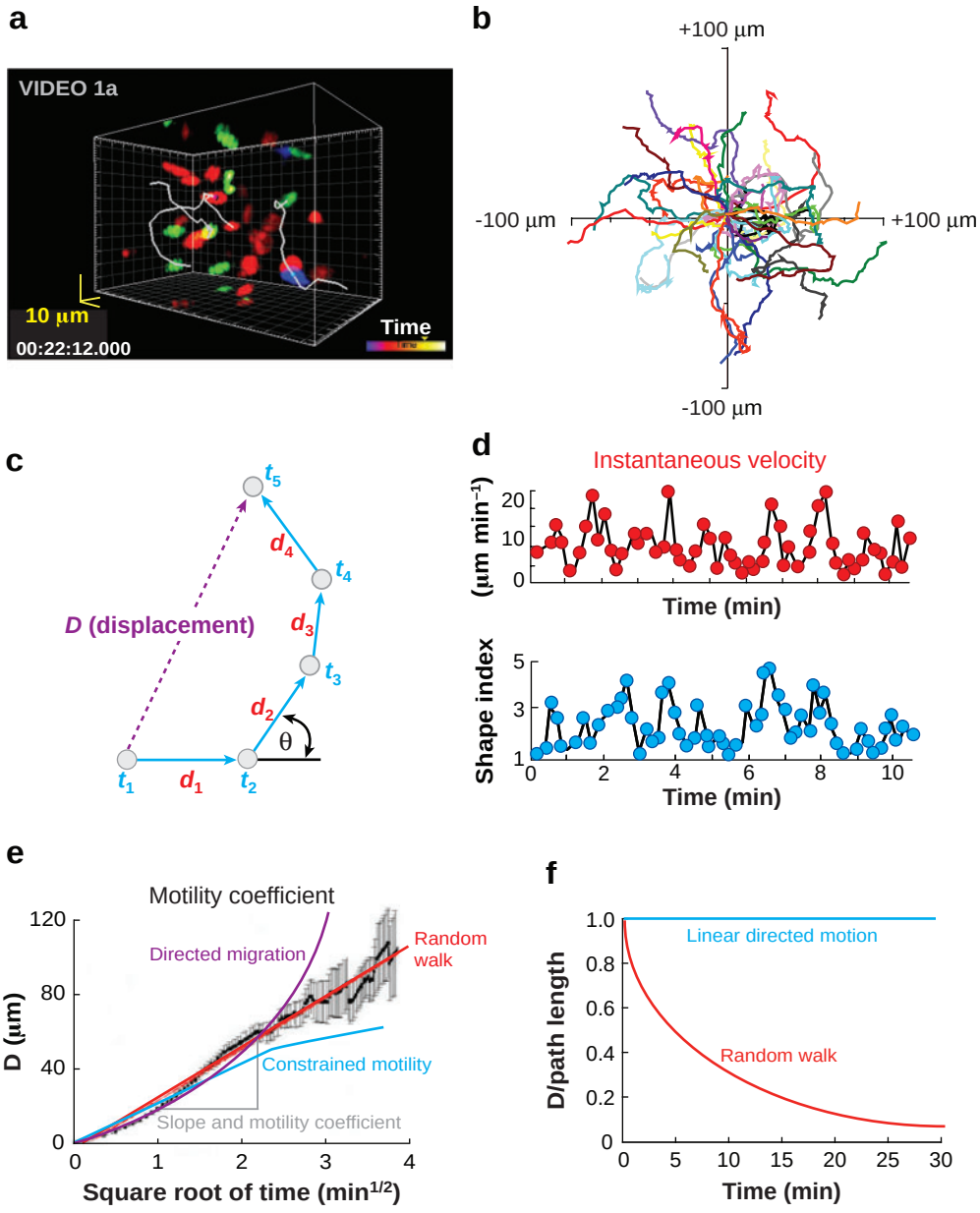

Table 1 Parameters used to characterize cell motility and migration

Parameter	Description	Unit
Instantaneous velocity (v)	Velocity calculated as displacement/time during a single time step	μm/min
Mean velocity (V)	Mean velocity of a cell over several time steps (usually the entire imaging period)	μm/min
Contact time	Time for which a cell is in contact with a defined cell or structure	sec: min
Shape index	Measure of cell polarization (long axis/short axis)	
Path length	Cumulative distance traveled by a cell over a given time	μm
Displacement (D)	Straight-line distance of a cell from its starting point after any given time	μm
Motility coefficient (M)	$M = \text{displacement}^2/4t$ (for 2-D measurements) or $\text{displacement}^2/6t$ (for 3-D measurements); analogous to the diffusion coefficient for Brownian motion	μm^2/min
Chemotactic index	Displacement/path length for a given time interval (a measure of cell directionality)	
Turning angle	The angle through which a cell deviates between successive time steps	degrees
Persistence time (length)	Time (length) for which a cell continues moving in a straight line before making an appreciable turn	min (μm)

practical difficulty with this method is that cells exit the imaging volume at longer times, resulting in increasing standard error as fewer cells remain and possible bias as the remaining cells are likely to have lower velocities. Deviations from linearity of the displacement versus square root time plot point to nonrandom processes (**Figure 1*e***): (*a*) At intervals shorter than the persistence time, the relationship will curve upward, as cells migrate without turning; (*b*) transition from a linear relationship to a plateau is consistent with migration confined by physical or biological barriers; (*c*) a steeper-than-linear slope indicates directed motion (27). The motility coefficient is a function of both the directionality of motion and the cell velocity, whereas the chemotactic index (displacement/path length) provides a measure of

Figure 1

Basics of motility analysis. (*a*) Snapshot visualization of the 3-D locations of fluorescently labeled cells throughout the imaging volume at a single time point. Tracks of three cells are superimposed. The cells are CFSE-labeled allogeneic $CD8^+$ T cells (*green*), CMTMR-labeled allogeneic $CD4^+$ T cells (*red*), and CMF2HC-labeled syngeneic $CD4^+$ T cells (*blue*) in the lymph node of B6D2F1 (H-2b/d) mice (**Video 1a** provided by Y. Yu). The total volume is (86 μm × 57 μm × 50 μm). (*b*) Flower plot representation of 2-D tracks of several cells, superimposed after normalizing their starting coordinates to the origin (adapted from Reference 26). (*c*) Schematic showing the track of a cell at five successive time points, t_1, t_2, etc. Instantaneous velocities are calculated from the net distance *d* traveled during each time interval Δt, and the turn angle θ is the angle through which the cell turns between time steps. The displacement *D* is the straight-line distance of the cell from its origin at any given time. Path length is given by the sum of d_1, d_2, d_3, etc. Persistence time (or length) is the time for which a cell continues to move without turning appreciably, as is illustrated for time points t_2–t_4. (*d*) The instantaneous velocity of T cells fluctuates in a characteristic manner over time, accompanied by changes in shape index (long axis/short axis) as the cell elongates while moving faster (adapted from Reference 2). (*e*) A plot of mean displacement from origin of multiple cells is expected to follow a straight line when plotted as a function of square root of time, if cell motility follows a random walk (adapted from Reference 26). The slope of this line can be used to derive a motility coefficient M, analogous to the diffusion coefficient for Brownian motion. Deviations from a straight-line relationship may be indicative of directed migration (upward curvature) or migration constrained by physical or biological barriers (plateau). (*f*) Chemotactic index. This measure, defined as path length/displacement from origin, remains constant with a value of unity for linear-directed motion but decreases progressively with time for cells following a random walk. Video may be viewed separately by following the **Supplemental Materials** link on the Annual Reviews website at **http://www.annualreviews.org**.

directionality that is independent of velocity but must be stated for some given time interval (**Figure 1*f***).

CELLULAR DYNAMICS WITHIN THE LYMPH NODE IN THE ABSENCE OF COGNATE ANTIGEN

Since the pioneering work of Gowans and colleagues (28–30), the processes of lymphocyte homing and tissue localization have been investigated extensively, resulting in our current understanding of how lymphocytes distribute from the blood to lymphoid organs and to peripheral tissues of the body (31–34). In the following sections, we review how two-photon immunoimaging allows us to visualize the dynamics of lymphocytes within the black box of their native tissues. Although the individual cellular components had been investigated previously in vitro, cell behaviors and the dynamics of cellular interactions turn out to be quite different within the complex tissue environment.

We first consider the behavior of T and B cells following homing to lymph nodes under basal conditions without antigen priming.

Basal Motility of T and B Lymphocytes

Early single-cell in vitro observation of living immune cells revealed their ability to crawl in an amoeboid manner on a variety of substrates (35–45). Yet many immunologists retained a view of resting lymphocytes as round, quiescent cells that somehow become more lively and energized in response to antigen.

In contrast, the first study to apply two-photon microscopy to the lymph node revealed rapid migration of T and B lymphocytes under basal conditions within a lymph node explant (2). T cells within the diffuse cortex migrate with about twice the average velocity of B cells in the follicle (10–12 μm/min versus 6 μm/min for 2-D velocities) and with a motility coefficient five- to sixfold higher for T cells than B cells. T and B cells are highly polarized while crawling, sometimes to an extreme of being four to five times longer than they are wide, and they move in a stop-and-go manner, with pauses between bursts, and reach peak velocities up to 30 μm/min for T cells and 20 μm/min for B cells. Tracking single cells revealed that T cells in the diffuse cortex and B cells in the follicle apparently move in random directions in all three dimensions. Rather than moving en masse, as might be expected if their migration were predominantly influenced by pervasive interstitial chemokine gradients, T and B cell tracks meander away from any arbitrary starting point in a manner reminiscent of molecules diffusing in solution. As a simple test for a random walk, plotting cell displacement as a function of the square root of time reveals an approximately linear function, as it would be for diffusion. Of course, the cells are not moving by diffusion but are crawling in an amoeboid manner. Miller et al. (2) labeled the reticular fiber network by soaking lymph nodes in CMTMR and observed T cells interacting with the labeled scaffold elements as well as T cells crawling over and interacting with each other. Subsequently, it has been shown that T cells migrate along a scaffold of fibroblastic reticular cells (FRCs) (25) that is associated with and extends beyond a network of resident DCs (22) near the cortical ridge adjacent to the B cell follicle.

There was initial concern regarding whether the rapid and random motility of lymphocytes in the lymph node explant accurately reflect their true in vivo behavior. Perhaps the disruption of lymph flow and blood circulation disturbed preexisting chemokine gradients that direct the migratory patterns of lymphocytes in the lymph node. Moreover, a contemporary report (3), using confocal microscopy of lymph node explants, described resting T cells as immotile. In retrospect, the primary reason for the latter difference is likely that T cells within the subcapsular sinus region of the lymph node are less motile than deeper cells (which are accessible to

two-photon, but not confocal microscopy) because in this region they lack chemokine signaling that enhances motility (46–48). These issues provoked a follow-up investigation using two-photon microscopy to examine naive T cell motility in an intravital preparation (26), exposing the inguinal lymph node in the anesthetized mouse. In the absence of antigen, naive T cells were again seen moving at 10–12 μm/min following a random-walk pattern within the diffuse cortex. Homing events were also visualized, as labeled T cells, imaged at 30 Hz and moving 1000 times faster in blood than in the interstitium, suddenly arrested at specific sites in the high endothelial venule (HEV), extravasated, and began to crawl through the interstitium of the diffuse cortex.

Together, these two studies by Miller et al. (2, 26) suggested an antigen-search strategy in which the purpose of rapid T cell migration is to locate and sample DCs for antigen within the relatively vast expanse of the diffuse cortex. Such a scanning mechanism could, in principle, solve the antigenic "needle in a haystack" conundrum of locating rare antigens without invoking specific attraction mechanisms. Moreover, the close agreement on quantitative measures of motility by several groups (22, 25, 26, 49, 50) confirms the robust motility of lymphocytes observed originally in the lymph node explant preparation (2), validating the lymph node explant preparation for further investigation of lymphocyte motility. There is now general agreement that the predominant macroscopic behavior of T cells in the diffuse cortex and of B cells in the follicle is rapid migration along apparently randomly oriented trajectories.

Lymphoid Architecture, FRCs, and Stromal Cell Guidance

Lymphoid organs are optimized for bringing together lymphocytes and antigen. T and B cells spend from 8 to 24 h in the lymph node interstitium before exiting by transiting across a lymphatic endothelium into a network of sinuses in the medulla that drain to efferent lymphatic vessels. While in the lymph node, T and B cells localize differentially to occupy distinct niches (**Figure 2*a***) within the diffuse cortex and follicles, respectively (51), guided by their differential expression of chemokine receptors (52). Although occupying distinct territory, T and B cells explore a very different landscape. Despite appearances from movies showing only fluorescently labeled lymphocytes, these cells do not migrate in a void. Instead, they crawl among a complex landscape of closely packed cells, including a vast excess of unlabeled lymphocytes, DCs, and stromal cells. Therefore, many factors may influence cellular motility in the complex environment of the lymph node.

The role of stromal cells in lymphocyte guidance has been clarified by Bajenoff and colleagues (25), who conclude that FRCs serve as a primary guidance scaffold for T cells in the diffuse cortex (**Figure 2*b***) and that follicular dendritic cells (FDCs) may fulfill the analogous function for B cells in the follicle. Bajenoff et al. (25) imaged in chimeric GFP mice that had been irradiated to destroy the endogenous fluorescent cells of the immune system, which were then reconstituted with GFP^- immune-precursor bone marrow cells. The resulting chimeras with an invisible immune system thus enabled intravital imaging of FRCs, FDCs, and vascular cells as GFP^+ cells in the lymph node. Although these cellular elements were well known by histological examination, the overall effect for live-cell immunoimaging was as if a previously invisible but extensive highway system were suddenly illuminated. In the T cell zone, the scaffold consists of a 3-D chicken-wire network of 5-μm thin $desmin^+$ $ERTR\text{-}7^+$ cells with 20- to 30-μm gaps between scaffold elements. Intravital imaging of red-labeled lymphocytes that were "salted in" as a random-sample survey revealed T cells crawling continuously along the FRC network, turning at branch points, and in rare instances jumping from one point on the scaffold to another, all the while making contact with scaffold elements

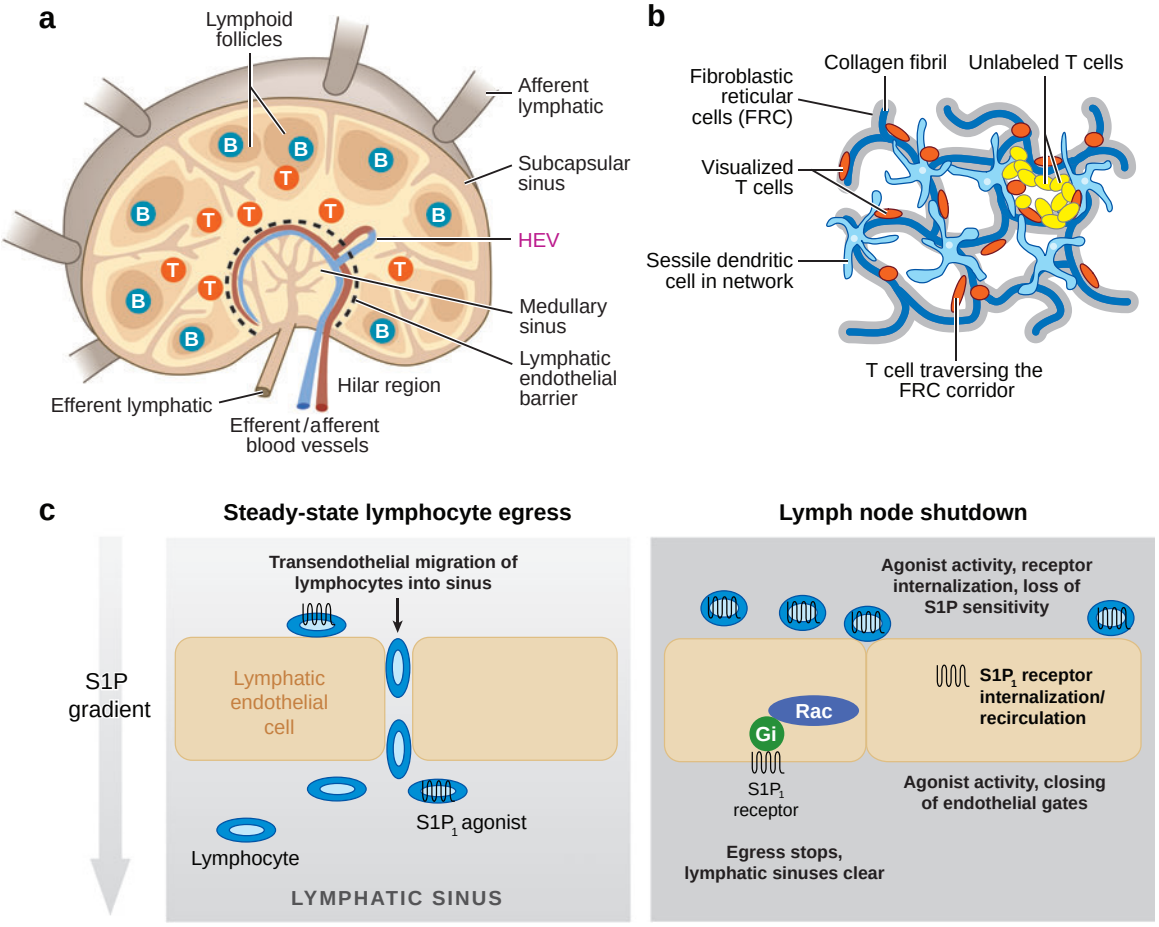

Figure 2

Structural and functional aspects of lymph node organization. (*a*) Macroscopic organization of lymph node regions, illustrating B cell follicles, T cell localization within the paracortex, and high endothelial venules (HEVs). (*b*) Schematic illustrating the motility of labeled T cells (*orange*) along and across the fibroblastic reticular scaffolding, in the presence of DC and an excess of unlabeled T cells (*yellow*), only a small fraction of which are shown in one region. (*c*) Hypothesis for regulation of lymphocyte egress by sphingosine 1-phosphate (S1P), illustrated under conditions of steady-state egress (*left*) and lymphopenia (*right*). T cells are shown with $S1P_1$ receptors either exposed or internalized in the presence of S1P. Junctions between the lymphatic endothelial cells close in the presence of an $S1P_1$ agonist.

like children on a jungle gym. Bajenoff and colleagues (25) also provided examples of T cell homing behavior, which had previously been imaged only in the absence of cellular landmarks (26). T cells enter the lymph node across HEVs and follow exit ramps to encounter a network of FRCs and DCs (25). Recently homed B cells also follow the FRC network until they reach the follicle, but within the follicle they migrate in contact with relatively sessile FDCs.

Simultaneous imaging of T cells with the stromal reticular network reinforces the importance of lymph node structural components that deliver antigen rapidly to the T cell zone and confirms ideas developed by Anderson, Shaw, and others on the basis of static imaging of histological sections (53–56).

FRCs and FDCs express the ligands ICAM-1 (intercellular adhesion molecule-1) and VCAM-1(vascular cell adhesion molecule-1), potentially providing an adhesive substrate for T and B cells, both of which express the corresponding integrins LFA-1 (lymphocyte function-associated antigen 1) and VLA-4 (very late activated antigen 4). The surfaces of FRCs and FDCs are decorated with differing chemokines bound to surface glycosaminoglycans. FRCs secrete the chemokines CCL19, CCL21, and CXCL12 and stain most strongly for surface-bound CCL21 in the paracortex (25, 57). CCL21 is a chemokine ligand of CCR7 on T cells. T cells have also been observed migrating directly in contact with resident DCs (22) that also express surface-bound CCL21 (58). The directionality of cells along a scaffold element is random, and thus movement along the scaffold is not guided by chemotaxis. In the next section, we review recent evidence strongly implicating haptotactic CCL21–CCR7 signaling to generally augment basal T cell motility. FDCs bear surface-bound CXCL13, the chemokine ligand of CXCR5 expressed by B cells. By analogy with the role of CCR7 on T cells, CXCL13 on the surface of FDCs acting on CXCR5 receptors may thus exert a similar influence on B cell motility in the follicle. The fidelity with which lymphocytes remain on the scaffold in the context of antigen challenge and molecular interventions will be intriguing to determine.

Signaling Pathways Regulating Basal Lymphocyte Motility

In their default state in the absence of antigen, lymphocytes are highly polarized in the lymph node and move more rapidly than other cell types. On the one hand, although it is well established that chemokine receptor expression regulates lymphocyte homing and cellular localization within the lymph node (34, 52, 59–62), the predominant random-walk pattern of T and B cells within their respective regions is inconsistent with what would be expected for chemotaxis, by which cells migrate collectively toward a source of chemokine. On the other hand, recent studies have clarified the role of chemokines in enhancing overall lymphocyte motility (chemokinesis), particularly when bound to substrates (haptokinesis), the manner in which chemokines are presented on stromal cell surfaces in vivo (43, 63). Several recent studies have begun to unravel the molecular requirements for lymphocyte motility within the lymph node (**Table 2**) by dissecting the signaling pathway that leads from chemokine to receptor (G protein–coupled receptor, or GPCR) to G protein and, ultimately, to the cytoskeleton. Some studies have focused on lymphocyte-extrinsic factors such as chemokines found in the lymph node environment, and others have focused on cell-intrinsic factors that include molecules or signaling pathways within the cell.

G protein–coupled receptor. Chemokines bind to heterotrimeric GPCRs to trigger downstream changes in lymphocyte polarity and migration. In particular, pertussis toxin–sensitive Gαi isoforms play a key role in homing and localization, and the chemokine receptors expressed by T cells (e.g., CCR7 and CXCR4) couple through Gαi. Three studies now indicate that Gαi may play a major role in promoting basal T cell motility in the lymph node (47, 57, 64) by showing that pertussis toxin inhibition of Gαi results in a decreased T cell velocity and motility coefficient (**Table 2**). Cells fail to migrate over long distances not only because they move more slowly, but also because they turn with broader angles. The $G\alpha_i$ subunit of heterotrimeric Gi exists in three mammalian isoforms. Genetic deletion of Gαi2 results in a smaller effect in B cells (65) than in T cells (66).

Chemokines and haptokinesis. Among the chemokine receptors that couple through pertussis toxin–sensitive Gi proteins, CCR7 has a substantive role in promoting T cell motility

Table 2 Molecular interventions and T cell motility in lymph node

Condition or treatment	Homing and Egress Rates	Velocity	Turning angle	Motility coefficient	References
Pertussis toxin	↓↓ homing	↓50%–60%	↑↑ (broader)	↓↓80%–90%	47, 57, 64
$G\alpha_i2^{-/-}$	↓ homing	↓30%–50%	↑		66
$CCR7^{-/-}$	↓ homing	↓20%–30%	↔[a]	↓50%–60%	47, 48, 64
CXCR4 antagonist or $CXCR4^{-/-}$		↔			57, 64
plt recipient mice	↔	↓20%–30%	↔	↓70%	48, 57, 64
$p110\gamma^{-/-}$	↓homing	↔	↑	↓16%	71, 72, 76
$p110\delta^{-/-}$	↔	N/A[b]	N/A	N/A	71
$p85\alpha^{-/-}$	N/A	↓12%	N/A	↓21%	70
$p85\beta^{-/-}$	N/A	↓26%	N/A	↓56%	70
$p85\alpha/p55\alpha/p50\alpha/p85\beta^{-/-}$	N/A	↓37%	N/A	↓78%	70
Wortmannin	↔	↓26%[c]	N/A	↓33%	70
		↔[c]		↔[c]	57[c]
$DOCK2^{-/-}$	↓ homing and egress	↓40% paracortex, ↓60% medulla	↑↑	↓93%	72, 76
DOCK2/p110γ	↓↓ homing and egress	Similar to $DOCK2^{-/-}$	↑↑	↓96%	72, 76
$CD18^{-/-}$ (lacking LFA-1)	↔	↓15%	↑	↓30%	63
$ICAM1^{-/-}$		↓25%			63
antiα_4 integrin		↓15%			63
MHC-II recipient after 7 days		↓70%			82
FTY	↓↓ egress	↔ in paracortex			47, 93
$S1PR_1^{-/-}$	↓↓ egress	↔ paracortex			93
S1PR antagonist	↔	↔ paracortex			84
		↔ medulla			
$S1PR_1$ agonist	↓↓ egress	↔ paracortex, ↓↓ medulla			84

[a]↔ No change.
[b]N/A Not applicable.
[c]Different conclusions in cited references.

in the lymph node. Four recent studies concur that $CCR7^{-/-}$ T cells show a 20%–30% reduction in T cell velocities (47, 48, 57, 64). CCL19 and CCL21, ligands for CCR7, both enhance motility of T cells when bound to substrates in vitro (43, 63). CCL21 is present in lymph nodes at much higher concentration than CCL19 (67) and is bound to the cell surface of both FRCs and DCs (57, 58). In recipient plt mice lacking CCL19 and CCL21, velocities of wild-type T cells are inhibited to a similar extent as in CCR7-deficient T cells (48, 57, 64), and motility of wild-type T cells in plt recipients recovers to normal following i.v. injection of CCL19 (48). Together, these results indicate that CCR7 plays an important role in enhancing T cell motility within the lymph node, with residual motility of cells perhaps reflecting chemokinesis mediated by another chemokine. Inhibition of CXCR4, using a specific antagonist or by genetic deletion, has no effect in wild-type T cells (57, 64), but one report (57) observed a further diminution of motility in CCR7-deficient T cells to a level comparable with inhibition by pertussis toxin. Thus, CCR7 appears to mediate an important chemokinetic effect on motility, with CXCR4 playing a possible secondary role.

Integrins and adhesion molecules. Cell adhesion molecules, such as ICAM-1 on stromal cells and APCs and integrins on T cells, are also thought to regulate lymphocyte motility (68), whereas their role in supporting basal motility in the lymph node may be surprisingly limited. A recent paper (63), combining in vitro and in situ imaging of lymphocytes, elegantly reveals the interplay between CCR7, the integrins LFA-1 and VLA-4, and shear stress on lymphocyte motility. Shear stress induced by solution flow over cultured cells rapidly causes arrest as a result of LFA-1 adhesion to ICAM-1 on the substrate (63). Such conditions are likely present in the vascular lumen, where integrins mediate the adhesive interaction that stops lymphocytes at sites of homing. Once inside the lymph nodes, however, shear stresses are absent, minimizing the adhesive function of LFA-1 interactions with ICAM-1. Consistent with this interpretation, Woolf et al. (63) further show that genetic deletion of LFA-1 in the donor T cell or ICAM-1 in the recipient lymph node has little effect on T cell motility, and blockade of VLA-4 using a blocking antibody has no additional effect.

Phosphoinositide 3-kinase. Among members of the phosphoinositide 3-kinase (PI3K) family, two major classes, IA and IB, are important in cell motility (69). Class IA and IB PI3K regulatory subunits include five and two isoforms, respectively, that, together with distinct catalytic subunits, are expressed in combinations of heterodimers in a tissue-specific manner. Two groups explored the possible involvement of PI3K activity in modulating lymphocyte motility by employing wortmannin as an irreversible inhibitor of all PI3K isoforms, but they reported divergent results. In lymph node slices imaged by epifluorescence microscopy, pretreatment with wortmannin had no effect on T cell motility (57). In contrast, recent work from our group, in collaboration with David Fruman (70), showed that wortmannin treatment resulted in a significant decrease in T and B cell motility in lymph node explants (**Table 2**). Although class IA and IB catalytic subunits (p110δ and p110γ, respectively) had previously been shown to be involved in lymphocyte chemotaxis and homing (71, 72), and p110γ is indispensable for neutrophil chemotaxis (73–75), p110γ deletion had only a minor effect on T cell motility and did not alter velocity or B cell motility (76). Among class IA regulatory isoforms, T cells lacking either p85α or p85β showed reduced velocities, with p85β deletion being more profound. Genetically targeting four class IA regulatory isoforms together produced an even more dramatic motility phenotype (**Table 2**), suggesting an additive effect (70). In B cells, regulatory isoforms may perform distinct functions, as p85α knockouts showed reduced velocity and displayed a striking, dendritic-like morphology, whereas p85β deletion had modest effects (70).

Dedicator of cytokinesis 2 (DOCK2). Guanine nucleotide exchange factors such as DOCK2 are centrally poised to communicate between GPCRs and cytoskeletal elements, and DOCK2 in particular plays a key role in lymphocyte homing, chemotaxis, and motility (72, 77). In lymphocytes, DOCK2 is required for Rac activation and actin polymerization and thus results in migration defects of lymphocytes (78). Similar to effects of pertussis toxin treatment discussed above, DOCK2-deficient T lymphocytes exhibit profound defects in lymphocyte motility (76) (**Table 2**), including a decrease in velocity and an even more severe decrease in motility coefficient resulting from increased turning angle. Similar defects are observed in B cells from DOCK2$^{-/-}$ mice. Double deletion of DOCK2 together with p110γ does not produce further changes, suggesting downstream mediation of DOCK2, but the possible interplay between DOCK2 and class IA regulatory isoforms of PI3K has not been examined.

Ca^{2+} ions and stop-and-go basal motility. The rise in cytosolic Ca^{2+} concentration triggered by T cell receptor (TCR) engagement

leads to gene expression required for lymphocyte activation. However, even in the absence of cognate antigen, intermittent Ca^{2+} signals occur in T cells as they migrate. In two recent studies (57, 79), Ca^{2+} was monitored during basal locomotion of T cells in lymph nodes. Ca^{2+} spikes lasting less than 2 min and rising sharply to a peak of about 200 nM are associated with temporary slowing of adoptively transferred T cells loaded with the Ca^{2+} indicator indo-1 and imaged in lymph node explants (79). In lymph node slices, Ca^{2+} spiking occurs in about 25% of T cells loaded with fura-2 and with higher frequency in arrested cells (57). Ca^{2+} spiking may be triggered by contact with DCs in the absence of specific antigen, and such intermittent spiking may play a role in cell survival, as it is less often observed in the absence of MHC class II in vitro (80). Such Ca^{2+} spikes do not, however, correlate well with the ongoing stop-and-go behavior of motile T cells.

MHC class II. Self-recognition mediated by contact with MHC class II is vital for T cell survival and proliferation in vivo (81). A recent study (82) showed that T cells deprived of contact with MHC class II in vivo by transferring OT-II T cells into MHC class II–deficient recipients become progressively immotile and disabled in their in vivo proliferative response to antigen. After seven days, T cells are essentially immotile. Biochemical analysis of T cells from mice treated in vivo with anti–MHC class II antibody, which deprives $CD4^+$ T cells of contact with self ligands, revealed a strong reduction in both active and total Rap1 and Rac1, but not in ras, suggesting a possible mechanism underlying the defect. The effects of MHC deprivation increase progressively, resulting in a diminished ability to proliferate from 30% after one day to complete inhibition within five days. The diminution in motility is likely not the sole cause of the decreased response to antigen but may contribute at later times, as motility is normal at intermediate times when activation responses had already declined substantially.

Temperature and tissue oxygenation. Lymphocyte motility is extraordinarily sensitive to experimental conditions. By common observation, lymphocytes stop moving if the laser power is too high, if excessive pressure is placed upon the lymph node, if the temperature is too low or too high, or if the tissue is not oxygenated, both in vitro and in vivo. The potential interplay between temperature and tissue oxygenation has been examined in greater detail using the lymph node explant preparation (47).

Regional Variations of T Cell Motility in the Lymph Node

Follicle edge. The trajectories of T and B cells at the edge of a follicle are decidedly nonrandom. There is a rather sharp divide of T cells outside and B cells inside the follicle, and cells migrating near the T-B boundary show relatively little mixing (83). Instead, most cells approach the edge and, without slowing, turn acutely and move back to join their compatriots. The occasional stray T cell that moves into the follicle and migrates among B cells maintains an average velocity typical of T cells in the diffuse cortex. Sharp segregation of T and B cells may be achieved simply by T and B cells remaining attached to their respective scaffold elements; Bajenoff et al. (25) show that most T cells straying into the B cell region still retain connection to FRCs. The important follicular edge, where helper T cells and B cells interact following antigen priming, is thus likely to be defined by overlap of follicular reticular cells.

Subcapsular sinus. T cells move with reduced velocity (35%–50%) and wider turning angles in the shallow subcapsular region of the lymph node (46–48, 66). These motility characteristics are similar to those of T cells in the paracortex in the absence of CCR7 or its ligands (**Table 2**). Indeed, the region of diminished motility in the subcapsular sinus correlates spatially with the absence of CCR7 ligands. Furthermore, subcutaneous injection

of the CCR7 ligand, CCL19, greatly enhances motility and numbers of wild-type, but not of CCR7-deficient, T cells in the subcapsular sinus (48).

Medulla. T cells in the medullary region near the hilus of the lymph node move more slowly than in the paracortex, with a 2-D velocity of 6 μm/min (76, 84). CXCL12 is enriched in the medulla (57, 85), but this chemokine, the ligand for CXCR4, does not induce chemokinesis in vitro (64) and does not affect motility in the paracortex.

Control of lymphocyte egress. Lymphocytes exit the lymph node by migrating from medullary cords across an endothelial barrier into efferent sinus vessels. A convergence of pharmacological (86, 87) and genetic evidence (88) indicates that sphingosine 1-phosphate ($S1P_1$) receptors regulate lymphocyte egress. In particular, FTY720 in its in vivo–phosphorylated form and related compounds that bind with high affinity and specificity to different Gi-coupled S1P receptors result in lymphopenia, as lymphocytes are trapped within secondary lymphoid organs (86, 87), and genetic targeting of $S1P_1$ receptors prevents lymphocyte egress (88). $S1P_1$ receptors are expressed on both lymphocytes and lymphatic endothelial cells, and there is continuing debate regarding the cellular targets and mechanisms regulating egress. Several recent reviews (52, 89, 90) discuss this topic. One school considers that lymphocytes migrate by chemotaxis toward a higher S1P concentration in the sinus lumen. The action of FTY720 is then explained by functional antagonism, whereby irreversible binding of FTY720 effectively removes $S1P_1$ receptors from the lymphocyte surface and degrades them, rendering lymphocytes blind to an S1P gradient. An alternative (not necessarily mutually exclusive) hypothesis implicates stromal gating by lymphatic endothelial cells. In this view, $S1P_1$ agonists engage endothelial receptors and close the gates through which lymphocytes migrate. Here, we focus on imaging data showing that agonist activity is required for pharmacologically induced sequestration.

Imaging of the egress step was first achieved in explanted nodes by orienting medullary sinuses on the hilar side toward the microscope (76, 84), and subsequently extended to intravital imaging (91). In the presence of a reversible $S1P_1$ receptor agonist that does not lead to receptor degradation (87, 92), medullary sinuses (visualized using a fluorescently conjugated lectin to stain the endothelial lining) are empty, whereas rounded and immotile lymphocytes become logjammed in the adjacent medullary cords. Removal of $S1P_1$ agonist, or addition of a molar excess of an $S1P_1$ receptor agonist in the maintained presence of agonist, results in rapid resumption of motility, with lymphocytes often crossing into the sinus at specific portals (84). A further key point is that neither the $S1P_1$ receptor agonism nor antagonism alter the robust motility of T cells in the paracortex of the node (**Table 2**), with the agonist action being restricted to the medullary region where basal motility is already lower (6 μm/min) than in the paracortex (10–12 μm/min).

Any model of egress and the role of S1P receptors under basal conditions must account for the following results: (*a*) Transendothelial migration occurs at preferential sites (portals) in the lymphatic endothelium (84); (*b*) $S1P_1$ receptor agonism induces actin polymerization in lymphocytes (76), potentially accounting for observed reductions in lymphocyte velocity in the medulla (84); (*c*) lymphocyte migration in the paracortex is unaffected by reversible $S1P_1$ or receptor-degrading agonists or antagonist (84, 93); and (*d*) reversible $S1P_1$ agonists that induce lymphocyte sequestration produce a rapid and region-specific motility arrest that is reversible upon removal of the agonist or addition of a stoichiometric antagonist (84, 91). We propose a hybrid model (**Figure 2*c***) in which both $S1P_1$ receptors in lymphocytes and lymphatic endothelial cells play a role. Intrinsic S1P agonism inhibits lymphocyte motility in a region-specific manner, constrained to the medullary cords where

CCR7-induced haptokinesis may be reduced. In the absence of agonist, the random motility of lymphocytes brings them to portals through which they transit into the lymphatic sinus system, where lymphatic flow returns them to the blood. As a further checkpoint, the portals are gated by $S1P_1$ agonist action.

Overview of Extrinsic Factors, Intrinsic Factors, and the Random Walk

Within the past two years, the roles of stromal cells and chemokines in lymphocyte motility within the lymph node have been clarified, and significant progress has been made in defining signaling molecules and pathways within the cell that are essential for motility (**Table 2**). Lymphocytes migrate along a stromal cell scaffold in which both FRCs and DCs display surface-bound CCL21. T cells, while crawling on FRCs that encapsulate the reticular conduits, make brief contacts with DCs to sample antigen along the way. T cell motility along the scaffold is enhanced by the chemokine CCL21 bound to the surface of FRCs. By haptokinesis, CCL21 binds to CCR7, which couples through the $G\alpha_i$ subunit of heterotrimeric Gi to enhance motility. When this function is disabled, T cells crawl with reduced velocity and broader turning angles, giving rise to highly localized cell tracks. In these instances, cell rounding of normally polarized T cells may reduce their ability to traverse adjacent elements of the scaffold, resulting in confined motion and greatly reduced motility coefficients. Class IA PI3K regulatory isoforms and DOCK2 mediate important effects on motility, but their links to chemokine receptors and downstream cytoskeletal effectors have not yet been fully defined.

A picture is thus emerging that the random walk of T and B cells in their respective compartments is guided and reinforced by haptokinetic signals obtained from stromal cells, and possibly also by DCs, and is mediated by chemokine receptor signaling through G proteins. To some extent, the stop-and-go program of motility may be intrinsic to lymphocytes because similar motile behavior occurs, albeit at lower velocity, even on a clean glass coverslip. Yet, there is no doubt that extrinsic factors enhance and guide motility in the lymph node environment. At the single-cell level, lymphocyte motility is not autonomous but rather is constrained by the scaffold that provides guidance cues as well as haptokinetic help via chemokines acting on GPCRs. From a systems perspective, however, the resultant motility patterns resemble swarm intelligence, by which the dynamic and seemingly autonomous motility of lymphocytes serves collectively to promote exploration of the interstitial lymphoid space and detect antigens. In addition, stromal guidance calls into question the role of chemokine gradients in guiding localization of T and B cells into separate compartments within the lymph node. If stromal cells are "rulers over randomness" (94), the exclusion of T lymphocytes from the follicle may depend on the distribution of FRCs, rather than on localized chemotaxis at the edge of the follicle. In this view, the issue of lymphocyte localization has been pushed back developmentally to the question of what limits the extent of FRCs and FDCs that form the respective scaffolds for T and B cells. B cells are more promiscuous in crawling both on FRCs soon after homing and among FDCs once inside the follicle. Further tests of the possible role of local chemokine gradients and stromal guidance at the edge of the follicle will rely on a more detailed analysis of cell behavior in this region and the ability to perturb local chemokine gradients. **Figure 3** provides a visual representation, with videos available online, of basal motility in the lymph node in the absence of antigen.

Migration and Dynamics of DCs

DCs initiate immune responses by capturing, processing, and presenting antigen. More than 60% of T cells in the lymph node are thought to be contacting a DC at any

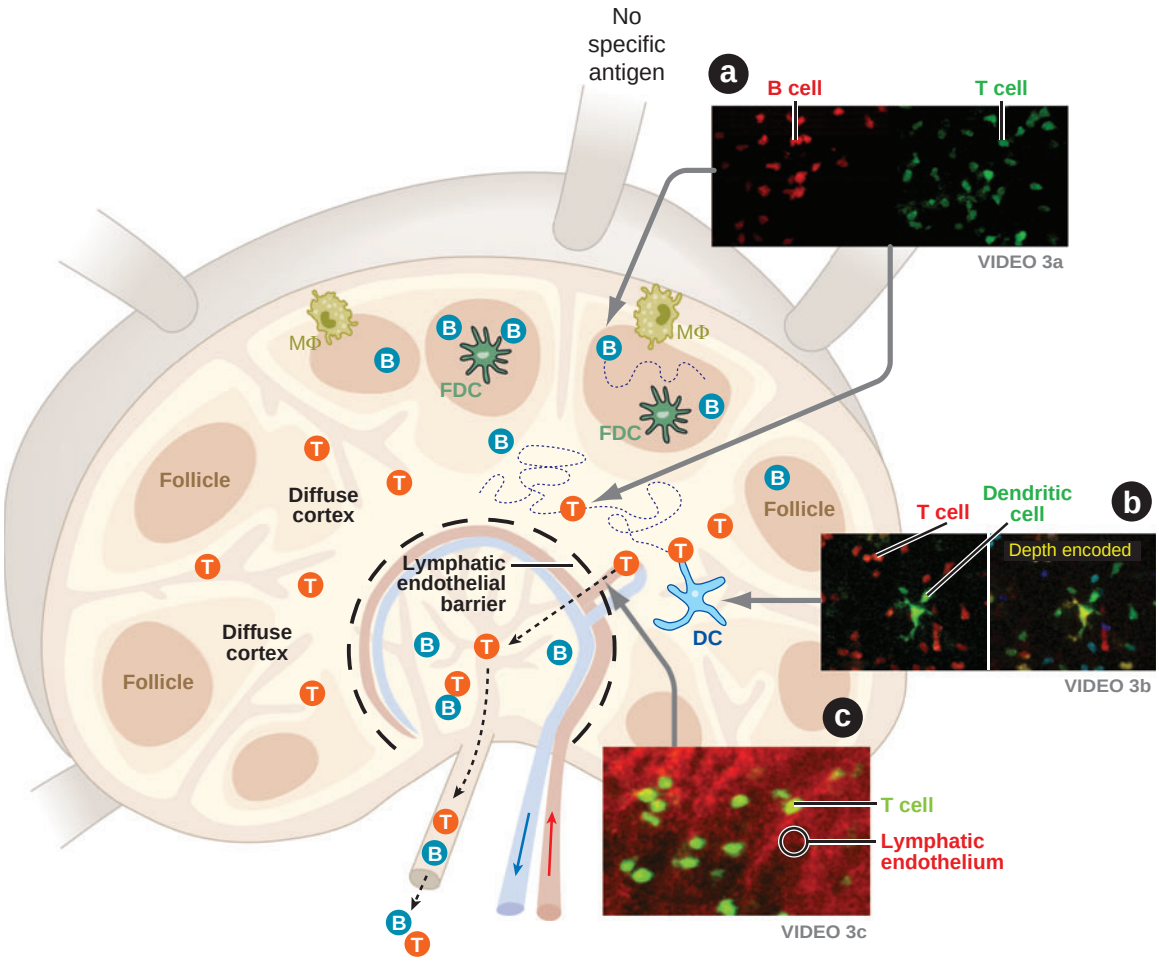

Figure 3

Cell motility and interactions in the absence of antigen. T and B cells are depicted migrating randomly in diffuse cortex and follicles, respectively. A recently homed B cell is on its way toward the follicle. Macrophages and FDCs within the follicle are devoid of specific antigen. A T cell is shown interacting transiently with a resident DC, while another T cell crosses the lymphatic endothelium to gain access to the efferent lymphatic vessel. Shown on right are frames from **Videos 3a, 3b,** and **3c,** respectively: (*a*) Montage of T cell and B cell dynamics, imaged separately in their respective regions (2); (*b*) T cells interacting transiently with a DC (96) (panel on the left is a "true" color maximum intensity projection along the *z*-axis and that on the right shows the same sequence after color depth encoding); (*c*) T cells migrating across the lymphatic endothelium (endothelial cells are stained with red fluorescent lectin) (84). Videos may be viewed separately by following the **Supplemental Materials** link on the Annual Reviews website at **http://www.annualreviews.org**.

time (95). Steady-state and freshly migrated Langerhans-derived DCs populate the entire diffuse cortex of the lymph node, whereas newly immigrated dermal DCs localize to the cortical ridge, adjacent to reticular conduits for efficient antigen capture and also near HEVs to favor encounters with newly homed T cells. Resident DCs are in intimate contact with FRCs that surround the reticular conduits, and both cell types bear surface-bound CCL21 (25, 58). Networks of $CD11c^+$ steady-state DCs have been visualized using

two-photon microscopy (22). Resident DCs are sessile, but long and active dendritic processes actively probe passing motile T cells. Freshly migrated DCs carry antigen from the periphery and dynamically traverse the diffuse cortex of the draining lymph nodes, often approaching the cortical ridge, and continually scan T cells with actively probing dendrites (49, 96). FDCs are not of hematopoietic lineage. These radiation-resistant stromal cells populate B cell follicles and have a high capacity to capture and retain antigen in the form of immune complexes (97–99). Imaging of FDCs by Bajenoff et al. (25) shows them to be stationary but displaying irregular and highly motile strands. While migrating in the follicle, B cells extensively contact the cell body and strands of FDCs. FDCs have also been imaged in germinal centers (21).

Natural Killer Cells: Stationary or Motile?

Although sparse in lymph nodes (<0.5% of total cell count), natural killer (NK) cells serve distinct roles in both innate and adaptive immunity (100) and are mobilized during infection and transplantation to produce cytokines and directly kill virus-infected or foreign cells. They are strategically poised to influence antigen-specific responses during parasite infection, tumor rejection, and transplantation (101, 102). Two studies have now imaged NK cells in lymph nodes (103, 104). Bajenoff and colleagues (103) isolated NK cells by magnetic bead selection using CD49b, an α2 integrin with affinity for collagen. Imaged in the paracortex, these positively selected NK cells are scarcely motile, averaging less than 3 μm/min (in contrast to highly motile T cells moving three- to fourfold faster in the same region), and form prolonged contacts with both resident and newly arrived DCs. During *Leishmania* infection, NK cells are recruited from the blood, resulting in a tenfold increase in NK cell numbers in the lymph node, and localize primarily under and between B cell follicles. Here, a substantial fraction of interferon (IFN)-γ-producing cells (80%) are $CD49b^+$ NK cells in close proximity to DCs and $CD4^+$ T cells undergoing activation. Again, the NK cells responding to *Leishmania* infection and interacting closely with DCs are immotile. Localized IFN-γ secretion by NK cells in close proximity to resident DC networks could alter DC maturation and promote a Th1 polarized response (100).

A very different view of NK cell motility in the lymph node emerged from a study utilizing NK cells from $RAG^{-/-}$ donors in order to avoid the need for positive selection (104). These untouched NK cells localize to the paracortex, consistent with the previous study (103), but they are highly motile (6–7 μm/min) along randomly oriented trajectories (104). To resolve the apparent discrepancy in cell motility with the earlier report, Garrod et al. (104) showed that in vitro cross-linking of CD49b in the positive selection procedure renders the $RAG^{-/-}$ NK cells immotile following subsequent transfer and homing into lymph nodes. Positively selected NK cells have increased adherence to collagen, and immotile NK cells are found in the lymph node attached to collagen fibers, whereas unmanipulated NK cells migrate rapidly along collagen fibers. These findings sound a cautionary note about potential effects of positive selection on cell motility and, more generally, on other cellular responses studied following cell isolation. It will be of interest to track NK cell behavior in a more collagen-rich environment such as the skin, where these cells are mobilized in psoriasis or transplant.

CELL DYNAMICS AND INTERACTIONS DURING ANTIGEN ACQUISITION AND RECOGNITION

Dramatic changes in cellular choreography accompany the initiation of an immune response to a specific antigen. Although the immune response usually begins and ends in the periphery at sites of infection or immunization, the lymph node functions as a crucial

filter to capture, concentrate, and deliver antigens and as a site where cells interact to make decisions about whether to secrete cytokines, proliferate, and differentiate. It is now clear that very different mechanisms are employed to deliver antigens to T cells than are used for antigen capture by B cells. Moreover, a very different cellular choreography takes place for T and B cells when they are activated (**Figure 4**). Focusing primarily on recent

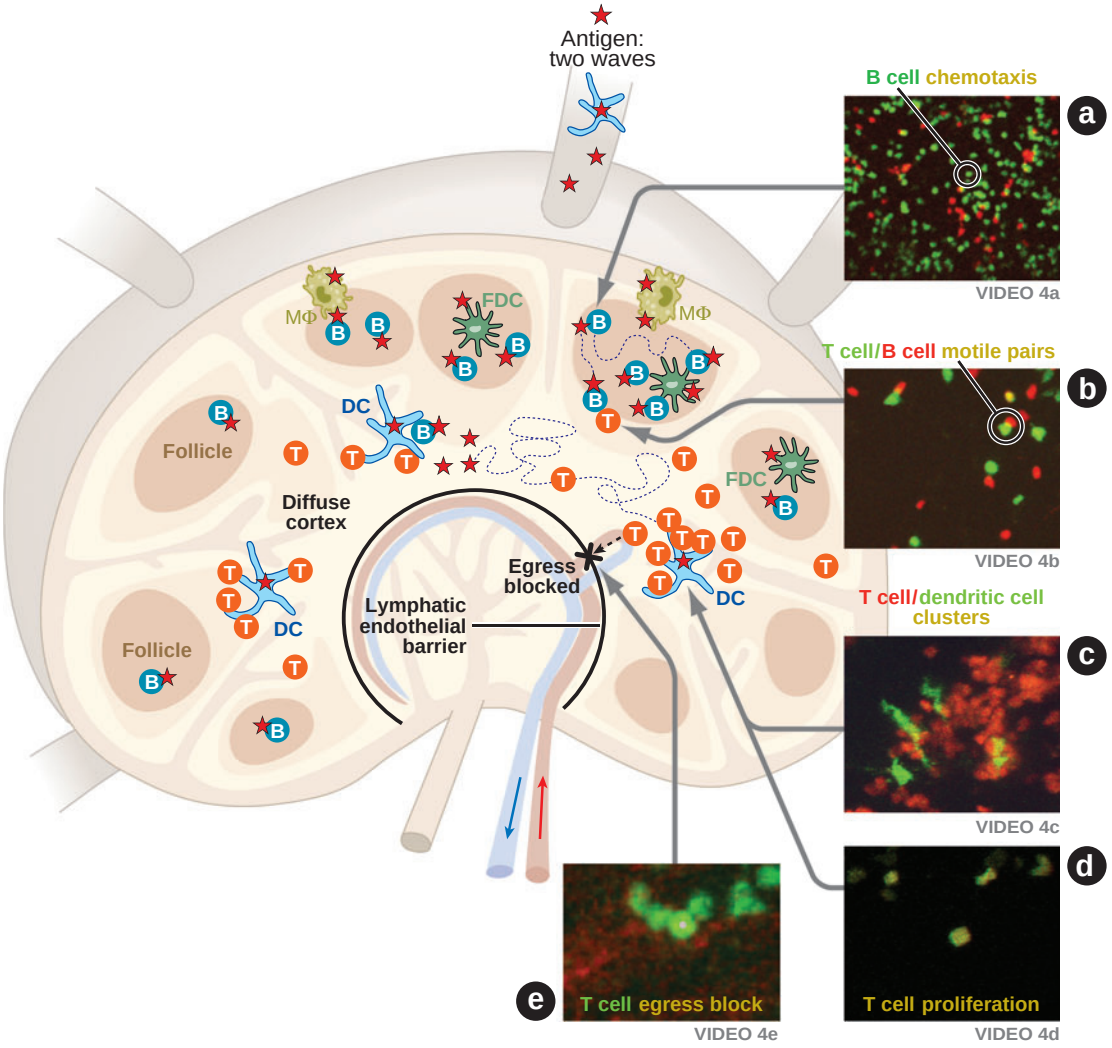

Figure 4

Cellular choreography with antigen. B cells move by chemotaxis to the follicle edge, after picking up antigen from macrophages and from FDCs. A T cell/B cell conjugate pair is shown at the edge of a follicle, together with T cells clustering around a dendritic cell bearing cognate antigen. T cells proliferate at this time, and egress is blocked. Shown on right are frames from the following videos: (*a*) B cell chemotaxis (146); (*b*) T cell/B cell motile pairs (146); (*c*) T cell/DC clustering (84, 117); (*d*) stereo movie of T cell proliferation (26); (*e*) egress block and subsequent recovery following removal of $S1P_1$ agonist at lymphatic barrier. **Video Links 4a–4e** may be viewed separately by following the **Supplemental Material** link from the Annual Reviews home page at **http://www.annualreviews.org**.

cellular immunoimaging studies, we follow in sequence the diverse routes by which antigen enters the lymph node; the cellular interactions between T cells and antigen-presenting DCs (close encounter of the first kind); and then the B cell side of the story as B cells become activated, interact with helper T cells (close encounter of the second kind), and differentiate in germinal centers to become antibody-secreting plasma cells.

Antigen Acquisition

Antigen delivery to and capture by DCs. Pioneering static imaging studies showed that the delivery of soluble antigen from the periphery via afferent lymphatic vessels into the lymph node occurs in two successive waves (105). Soluble antigen arrives first, conveyed rapidly within reticular conduits (106), and is then taken up, processed, and displayed as peptide-MHC (pMHC) by resident DCs within 30 min (105). A second wave of antigen, borne by dermal-derived DCs from the skin, subsequently arrives a few hours later. Live cell imaging in the skin shows epidermal CD11c$^+$ Langerhans cells (langerin$^+$) and deeper, immature dermal DCs (107) as being entirely immotile cells with stationary dendrites under basal conditions. After triggering by inflammatory cytokines and by activation of Toll-like receptors (TLRs), Langerhans cells and dermal DCs migrate to the lymph node via afferent lymphatic vessels in a process that requires upregulation of CCR7 by DCs and CCL21 by lymphatic endothelial cells (108); this process has not yet been visualized.

The maturation of DCs and their cellular journey in afferent lymphatic vessels impose a delay of several hours, and CFSE-labeled migratory DCs are first visualized following their arrival in the lymph node more than 4 h after subcutaneous injection, together with adjuvant-containing cytokines to induce maturation (96). Their numbers increase during the next day and then decline after two days in the lymph node. In an adjuvant depot, diffusion of soluble antigen away from the site of immunization is limited, and local capture by DCs followed by migration into the lymph node will dominate. The chemical composition of the adjuvant can also polarize a subsequent response by triggering different TLRs on DCs to promote subsequent Th1 or Th2 differentiation (109, 110). Different TLR agonists are known to differentially regulate the production of DC-derived IL-12, thus skewing Th1 or Th2 responses (109). Soluble antigen can use both routes, arriving passively within minutes or being conveyed as pMHC by tissue-derived DCs.

Antigen capture and delivery to B cells, and by B cells to FDCs. Antigen enters the lymph node in differing forms and by various routes. A recent study by Pape et al. (111) focuses attention on the rapid response capabilities of follicular B cells to capture soluble antigen entering the follicle. Following subcutaneous injection, soluble antigen arrives in the lymph node follicle by diffusion across small gaps in the floor of the subcapsular sinus directly to nearby follicular B cells, even faster (within a minute) than it is transmitted by reticular conduits into the T cell area. Such rapid delivery of soluble antigen from the subcapsular sinus to the interior of the follicle was not seen previously (55, 105, 106), perhaps because soluble antigen was washed away during fixation. The subsequent spread of antigen into the follicle interior proceeds more rapidly than B cells can migrate, indicative of passive diffusion. Within 10 min, all the antigen-specific B cells in the follicle have taken up antigen, and by 4 h, the antigen is processed and presented bound to MHC by B cells with greater efficiency (more antigen acquired) than by DCs in the paracortex. DCs do not play a role in the acquisition of soluble antigen by B cells.

To sustain the response to antigen, mechanisms for storage, sustained release, and delivery are also in place at the boundary of the subcapsular sinus and within the follicle. The subcapsular boundary functions as a sieve, restricting passive diffusion of larger forms of

antigen, such as that contained in immune complexes or bacterial particles. Two recent live-cell imaging studies (23, 112) show that antigen-trapping cells in the subcapsular sinus capture and retain surface-bound antigen. Phan et al. (23) implicate the macrophages that span the border of the subcapsular sinus, showing them in the process of capturing fluorescently labeled immune complexes in the sinus lumen and handing off immune complexes to migrating B cells just inside the follicle. Unlike many other macrophages, those here are not highly phagocytic and do not rapidly degrade the antigen. Instead, they acquire and hold immune complexes on the luminal side of the subcapsular sinus and somehow convey them to the follicular face, where the cargo is displayed attached to long processes. Nonspecific B cells slow during contact with macrophages, pick up immune complexes, and then depart at the normal velocity of randomly migrating follicular B cells (2). Phan et al. (23) further show that the departing B cells display distinctive dendritic processes reminiscent of germinal center B cells and carry away noncognate immune complexes as cargo attached to the trailing uropod while migrating toward the follicle interior, where immune complexes are off-loaded to FDCs.

Antigen recognition is not involved in this transport process, which relies on complement receptors CR1 and CR2 in the B cell for initial capture of immune complexes (but not for the acquisition of dendritic morphology). FDCs have a high capacity to retain immune complexes bound to high-affinity FcγRIIB and complement receptors, so that B cells are relieved of the antigen burden by the time they leave the follicle. If cognate antigen is present in the immune complexes or is attached to a particle, the B cells pause longer near the macrophages as B cell antigen receptors (BCR) become engaged (23, 112), allowing them to pick up more antigen cargo. BCR engagement in turn triggers relocalization of the antigen-engaged B cell toward the T cell area. Antigen-specific B cells may also encounter, recognize, and pick up antigen carried by nonspecific B cells that recently visited the macrophages at the subcapsular sinus (23). Collectively, these mechanisms will preserve antigen load within the follicle and allow late-arriving B cells to participate in the antibody response.

A third mode of antigen capture by B cells takes place outside the follicle near the sites of homing. There, a DC that has acquired antigen arriving in the reticular conduit system not only processes and presents the antigen as pMHC recognized by T cells, but also displays whole antigen bound to the cell surface in a form that is recognizable by B cells. Qi et al. (113) show by intravital immunoimaging that B cells survey the DCs immediately after homing. If specific antigen is present, the B cells stall and capture some of the surface antigen from the DC. The fate of these B cells, having engaged antigen in a most unusual locale, is to remain extrafollicular, where they can interact with helper T cells.

Activation of T Lymphocytes

Antigen presentation: scanning the T cell repertoire. In the diffuse cortex, FRCs surround collagen fibers and a basement membrane, forming a reticular conduit for antigen (53–55, 106). The cortical ridge region just outside the follicle includes resident DCs near sites of lymphocyte extravasation across HEVs (56). In this region, T cells sample resident DCs for the presence of cognate peptide antigen bound to MHC. The second wave of antigen that arrives from the periphery carried into the paracortex by maturing dermal-derived DCs hours after antigen injection may have differing functional consequences.

Live-cell imaging reveals recently immigrated DCs to be highly active cells that localize to the cortical ridge close to HEVs. While migrating with an average velocity of 2–6 μm/min (3, 49, 96, 114), they rapidly extend and retract dynamic dendritic processes, thereby greatly expanding their scanning range to >60 μm from the cell soma

(possibly longer with nanotubes), and enabling DCs to contact many more T cells than if they were stationary. The effective swept volume covered by motile dendrites is about threefold larger than if DC were rounded (96). In the absence of antigen, individual DCs make contact with up to 5000 T cells per hour (96, 114), an astonishing rate of cellular interaction that is promoted by dynamic DC dendrites and robust T cell motility. Contacts occur primarily on DC dendrites, rather than on the cell body, with a surface contact area on the order of 10 μm^2 (96), comparable to that needed to trigger a T cell Ca^{2+} signal through presentation of TCR ligand on beads (115).

Interactions between T cells and DCs appear predominantly to involve random encounters, as T cells approach DCs without changing course and migrate away after brief contact at the same velocity as their arrival (96). Such randomly initiated, short-duration encounters followed by rapid departure avoids unwanted competition for DC surface space by irrelevant T cells that would accompany nonspecific chemoattraction. The measured frequency of interaction suggests that any given DC can probe hundreds of motile T cells within a few minutes. Miller et al. (96) thus proposed a stochastic mechanism of antigen scanning that allows T cells to survey DCs within the diffuse cortex by randomly initiated contacts and initiate activation responses within 6 h, provided that ~100 antigen-bearing DCs are present. However, in addition to random motility, we have also noted striking instances in which several T cells simultaneously migrate from different positions toward a particular DC (M.D. Cahalan, S. Wei, and M. Matheu, unpublished observation), raising the possibility of intermittent chemokine-mediated guidance—for example by puffs of soluble CCL19 emitted from DCs, consistent with a proposed role of this chemokine in scanning behavior (116).

Stages of T cell–DC interaction during the first day of an immune response. In contrast to the brief contacts between T cells and DCs in the absence of antigen, early reports described T cells forming long-lived (hours) contacts with adoptively transferred, peptide-pulsed DCs, with ten or more T cells clustered on a single DC (3, 114). Covisualization of T cells and DCs at different times during the first day of in vivo antigen priming subsequently dissected distinct stages of interaction leading to cell proliferation (49, 117). These stages may differ somewhat between $CD4^+$ and $CD8^+$ T cells. During the initial stage, both $CD4^+$ (117) and $CD8^+$ T cells (49) make transient, serial contacts with several DCs, encounters that are sufficient to trigger upregulation of the activation marker CD69. This first stage is shorter for $CD4^+$ T cells (2–4 h) (117) than for $CD8^+$ T cells (8 h) (49). Both long and transient $CD4^+$ T cell/DC encounters were seen during the first 2 h in our original study (96), but long-duration encounters were predominant in subsequent investigations by Shakhar et al. (50) and from our group in a study that incorporated Ca^{2+} imaging (79), possibly reflecting a greater quantity of antigen delivery in these later studies. After progression to the second stage, T cells are observed in dense clusters, with several T cells usually maintaining continuous contact with a single DC for >90 min (the usual limit for live-cell observation by two-photon microscopy). Although generally stable, clusters also exhibit dynamic changes, with DCs ripping T cells away from nearby DCs (96), suggesting one type of competition that could occur if a second wave of DCs arrived. This second, cluster stage is accompanied by IL-2 production, indicating activation of NFAT (nuclear factor of activated T cells)-dependent downstream signaling leading to gene expression. From 16–24 h after initially encountering antigen, enlarged T cells dissociate from DC clusters and begin to swarm in looping patterns around DCs in a localized region. During this third stage, T cells again form transient contacts with additional DCs and later begin to proliferate. Motile T cell blasts that had previously separated from DCs round up and divide within 20–30 min. The daughter

T cells are immediately motile with 2-D velocities of about 10 μm/min, and within five days T cells have divided up to eight times.

T cell Ca^{2+} signal during antigen recognition. Progressing beyond an initial phenomenological description of cell behavior in the lymph node, the next challenge is to understand how cell interactions and signaling cascades within the cell are integrated to promote various immunological outcomes.

Within a few seconds of TCR engagement, Ca^{2+} signaling is initiated by IP_3-induced Ca^{2+} release from the endoplasmic reticulum (ER) and is subsequently sustained by Ca^{2+} influx through store-operated Ca^{2+} release-activated Ca^{2+} (CRAC) channels. CRAC channels are formed by Orai1 multimers activated by STIM1; these STIM1 multimers function dually as the ER Ca^{2+} sensor and as the activator of CRAC channel activity (118–120). Ca^{2+} signals must exceed 500 nM for at least 1–2 h to drive gene expression via the calcineurin-dependent NFAT transcription factor pathway (121–123). The Ca^{2+} signal may be oscillatory, spike-like, or sustained in individual cells. The frequency and pattern of Ca^{2+} signaling is important for activating various transcription factor pathways in a differential manner (124, 125).

Although in vitro studies have revealed much about the molecular mechanism and patterns of T cell Ca^{2+} signaling that lead to downstream transcriptional activation, an important goal remains to monitor signaling in primary T cells within the physiological context of antigen presentation inside the lymph node. A recent paper (79) describes Ca^{2+} signaling in lymph node T cells under basal conditions, during nonspecific inflammatory conditions, and during antigen-specific responses. Under basal conditions, T cells migrate rapidly and have low cytosolic Ca^{2+}, showing only infrequent, small-amplitude Ca^{2+} spike activity associated with T cell slowing. Inflammation by itself reduces motility and nearly eliminates intermittent Ca^{2+} spiking without affecting average Ca^{2+} levels. Antigen priming reduces velocities further and evokes strong Ca^{2+} signaling activity (79), evident as irregular transients to >500 nM. Cells with the strongest Ca^{2+} signals are associated with the lowest velocities. Those T cells observed in direct contact with labeled DCs have more pronounced Ca^{2+} signals, but the initiation and termination of DC contacts are not clearly correlated with any change in Ca^{2+} signaling. T cell Ca^{2+} signaling continues even after detachment from all visible DCs. These results define the pattern of the Ca^{2+} signal in naive T cells during antigen presentation under physiological conditions as consisting of persistent and irregular spike activity. Using confocal microscopy and a nonratiometric Ca^{2+} indicator, Skokos et al. (126) detected Ca^{2+} signals associated with T cell slowing in freshly homed T cells interacting with DC that had taken up DEC-205-conjugated high-potency peptide under tolerizing conditions. Lower-potency peptides failed to elicit Ca^{2+} signaling, T cell arrest, and downstream proliferative responses, even though they elicited upregulation of CD69.

Together, these first two Ca^{2+} imaging studies (79, 126) in lymph node emphasize the involvement of Ca^{2+} signaling in producing T cell arrest, regardless of T cell priming or tolerization, and herald a new phase of imaging that incorporates intracellular signaling responses together with tracking cell behavior in relation to functional outcomes.

Stop signal. Calcium signaling during antigen recognition inhibits T lymphocyte motility in vitro (38, 127, 128). T cell motility in vitro is also inhibited by elevated Ca^{2+} when proximal TCR signaling is bypassed by the use of Ca^{2+} ionophores or by treatment with thapsigargin. Immunoimaging of T cells, B cells, and thymocytes indicates that the Ca^{2+} stop signal hypothesis also applies in vivo. Intermittent Ca^{2+} signaling in the absence of antigen is sufficient to reduce the velocity of T cell migration (57, 79). Furthermore, T cells

and B cells produce Ca^{2+} signals and slow at sites of interaction with antigen-bearing DCs (79, 113). The most rigorous test was performed by Bhakta et al. (129), who showed that Ca^{2+} signaling is both necessary and sufficient for thymocytes to stop crawling in the thymic environment. Importantly, by changing the concentrations of Ca^{2+} and K^{+} ions in the medium, Bhakta et al. were able to restore the motility of arrested thymocytes by reducing Ca^{2+} influx. Using thapsigargin treatment, they showed that moderate Ca^{2+} levels stop cells reversibly, proving sufficiency. Lowering Ca^{2+} levels also inhibits Ca^{2+} signaling in a selecting environment and results in the resumption of motility, proving necessity. Like T cells interacting with APCs, the Ca^{2+} dependence of thymocyte motility prolongs interactions with stromal cells and promotes sustained Ca^{2+} signaling that in turn alters gene expression critical for deleting autoreactive thymocytes. Further validation of the Ca^{2+} stop signal hypothesis was obtained in recent work by Skokos et al. (126), who showed in the lymph node that, even under noninflammatory conditions, T cells decelerate and produce Ca^{2+} signals when responding to YFP-expressing DCs primed with the most potent in a series of altered peptide ligands. Together, these studies support the conclusion that Ca^{2+} signaling both in vitro and in vivo promotes the stability of T cell–APC interactions, an essential prerequisite for stabilizing the immunological synapse and downstream effector function.

A potentially important new wrinkle in the stop signal hypothesis has been raised by Schneider et al. (130), who report that CTLA-4 (cytotoxic lymphocyte antigen-4) increases basal T cell motility and overrides the TCR-induced stop signal required for stable conjugate formation between T cells and APC. CTLA-4 is well known as an inhibitory coreceptor on T cells that is induced upon activation and opposes costimulation by APC proteins CD80 and CD86 delivered to CD28 on the T cell. After separating CTLA-4^{+} and CTLA-4^{-} cells among a preactivated pool of antigen-specific T cells, the authors distinguished their motility and response to subsequent antigen challenge. In the lymph node, CTLA-4^{+} cells do not arrest during antigen challenge, suggesting that CTLA-4 expression prevents cell arrest during contact with antigen-presenting DCs. On the basis solely of differences in T cell behavior, one may conclude that the differences in cell arrest between these preactivated populations are due to a lack of initial antigen recognition by CTLA-4^{+} cells and to a corresponding suppression of the Ca^{2+} signal to below what is needed for cell arrest (131).

Antigen Quality, Quantity, and Timing

The initial descriptions of T cell–DC interactions (3, 49, 96, 114) have been extended in several studies that examined the consequences of varying conditions that alter T cell/DC dynamics and functional outcomes. When one considers the demonstrated effects of costimulatory signaling; antigen quality, quantity, and persistence; competition between cells for antigen; and timing of T cell and DC arrival to the lymph node, the potential complexities are enormous. Late T cell/DC encounters may provide a rationale for prolonging the stay inside a lymph node. During the days-long period of egress block (lymph node shutdown) during an antigen response, T cells may encounter DCs again and again to integrate signals delivered by successive waves of DCs migrating from the periphery. How these signals are integrated remains to be seen, but antigen persistence during the final days in the lymph node can also modulate T cell differentiation programs. Experiments tracking CD4^{+} T cell proliferation revealed that the presence of antigen throughout their expansion phase is essential for optimal activation (132). Furthermore, T cells induce antigen loss from the surface of DCs, resulting in high-affinity T cells outcompeting lower-affinity T cells during a response to antigenic challenge (133).

Tolerance and Priming. Three studies imaged T cell–DC interactions under conditions that produced either priming or tolerizing immune responses (50, 134, 135). In a priming response, initiated usually by antigen in combination with an adjuvant containing TLR ligands such as lipopolysaccharide (LPS) to promote DC maturation, the subsequent exposure to antigen induces a more rapid and robust functional response, whereas a tolerizing regimen using antigen alone results in a diminished functional response. Hugues et al. (134) and Shakhar et al. (50) used DEC-205 (to facilitate antigen uptake by steady-state DCs) conjugated to ovalbumin in the presence or absence of LPS or anti-CD40 (mimicking DC costimulation) to induce priming or tolerance. Hugues et al. (134) found that in the tolerizing regimen, $CD8^+$ T cells slow but do not arrest to the same degree during stage II as during priming. Differing from these results on $CD8^+$ T cells, Shakhar et al. (50) found that $CD4^+$ T cells arrest equally well in response to priming and tolerizing regimens but become more motile sooner during tolerization (at 18 h) compared with priming (at 24 h). Comparing oral priming with oral tolerance induction, Zinselmeyer et al. (135) found only minor differences in $CD4^+$ T cell motility and clustering behavior, with larger and more stable clusters seen in the priming regimen. Common themes among all three studies are that priming and tolerizing routines do not lead to markedly different T cell behaviors, but that priming is associated with more prolonged and/or more stable cluster formation during stage II. Such subtle differences in T cell–DC interactions could influence or reflect costimulatory signals delivered during the interaction.

The quality and context of pMHC presentation also matter. Skokos et al. (126) compared the dynamics and functional outcomes of steady-state DCs presenting high-, medium-, or low-potency pMHC complexes varying by only a single amino acid substitution in the peptide antigen conjugated with DEC-205 under tolerizing conditions. All three peptide ligands induced CD69 upregulation and anergy, but only high-potency MHC complexes resulted in Ca^{2+} signaling, T cell arrest, and stable T cell–DC interactions that subsequently led to the strongest proliferative response and cytokine production. These latter responses, but not CD69 upregulation, were inhibitable by cyclosporin A. However, CD69 upregulation induced by low- and medium-potency pMHC was shown to be sufficient to produce T cell anergy that is not inhibited by cyclosporin A, suggesting that anergy can be induced by Ca^{2+}-independent events that are activated during hit-and-run contacts with DCs. Together, these results emphasize the importance of stable T cell–DC interactions, during which effective Ca^{2+} signaling can take place, for proliferative responses and cytokine production in vivo.

Timing of DC arrival: sustaining the response. During the third stage of antigen presentation, $CD4^+$ T cells resume their motility and swarm away from their clusters while making contact with additional DCs (117). The consequences of a subsequent late encounter with an additional wave of DCs have been evaluated by Celli et al. (136), who sent in reinforcements, i.e., antigen-bearing DCs, during an already developing immune response. Swarming T cell blasts found and reengaged this fresh set of recent DC immigrants, sometimes again forming long-lasting contacts. Activated T cells that reengaged fresh antigen-bearing DCs did not proliferate to a greater extent but were more likely to express the high-affinity IL-2 receptor CD25 and to secrete IFN-γ. As this cytokine secretes directionally into the immunological synapse (137), it may exert a localized effect on the DC. These results on $CD4^+$ cell behavior differ from findings in $CD8^+$ cells rechallenged with antigen; in the latter case, $CD8^+$ cells did not reengage in long-lasting contacts following antigen delivered as a second wave at 20 h (134).

Timing of T cell arrival: competition and antigen persistence. Using static methods and by blocking homing to inhibit the arrival of T cells, Catron et al. (138) compared outcomes for resident and late-arriving T cells that entered the lymph node after a specific antigen response was already underway. Although this was not imaged, the late arrivers engaged DCs that presumably would have already accumulated T cell clusters. Tracking the outcome of residents and late arrivers separately showed that competition results in a weaker proliferative response among the late arrivers and predestines them to become central memory T cells. The resident T cells that benefit from the full antigen load have a greater tendency to become fully differentiated effector cells.

Garcia and colleagues (139) extended the theme of competition by sending in labeled T cells either alone or accompanied by a tenfold excess of identical but unlabeled cells. With low numbers of cognate T cells, competition for antigen-presenting DCs is reduced and the specific T cells form stable interactions with antigen-pulsed DCs for a longer period. At higher densities, competition among antigen-specific T cells for space on the DC surface is not limiting because the frequency of transient interactions with DCs increases when more cognate T cells are transferred. On a per cell basis, however, CD69 is less efficiently induced. As a direct test of whether the quantity of antigen is the limiting factor, i.v. injection of the peptide antigen restores long-duration late contacts 2 days after the initial exposure of antigen. Thus, competition for the quantity of antigen plays an important role in determining the stability of T cell/DC contacts and the duration of the second stage of stable T cell/DC clustering. The results emphasize that the initial phase of T cell expansion is limited by the quantity of antigen present. Furthermore, they imply that under the normal condition of low cognate T cell frequency, longer-duration conjugate T cell–DC interactions will form. As T cell expansion continues, competition for residual antigen by T cells becomes self-limiting. The late-arriving T cells that have a greater likelihood of becoming central memory cells (138) may do so because they endure competition for antigen by early arrivers which are more likely to become fully differentiated effectors.

Another form of negative feedback involves late-arriving cytolytic effector cells returning to the draining lymph node from the periphery. $CD8^+$ effector cells ($CCR7^-$ L-$selectin^-$) return by targeted homing specifically to draining lymph nodes in a CXCR3-dependent manner. Once inside the lymph node, these effectors were visualized making prolonged contacts with, and killing antigen-bearing DCs, thereby providing negative feedback by eliminating specific antigen-presenting DCs (140).

$CD4^+$ T Cell/$CD8^+$ T Cell/DC Ternary Clusters

During an immune response to whole antigen, both $CD4^+$ and $CD8^+$ T cells often become activated by contact with differing pMHC complexes on DCs. The activation of $CD4^+$ cells augments $CD8^+$ cell clonal expansion and differentiation to become memory and cytolytic effector $CD8^+$ cells (141). The initial recognition of antigen by either $CD4^+$ or $CD8^+$ T cells may be understood in the sense of a stochastic mechanism by which T cells make numerous random contacts with DCs, but the problem is compounded by the need to get all three cell types together. To investigate mechanisms of help provided by $CD4^+$ cells for the $CD8^+$ response, two groups examined the dynamics of $CD4^+$ and $CD8^+$ T cells interacting with DCs during responses that engage both T cell subsets. Each group imaged ternary clusters with both $CD4^+$ and $CD8^+$ cells in direct contact with antigen-bearing DCs (142, 143). Clustering of $CD8^+$ cells to DCs is enhanced by the presence of $CD4^+$ cells that recognize their cognate peptide on the same DC. Notably, this tripartite interaction is diminished by several molecular interventions: blocking

antibodies directed against either CCL3 or CCL4 (chemokines that are produced by T cells and DCs following their engagement); CCR5 genetic deletion in $CD8^+$ T cells; and DCs lacking CD40. The assembly of the ternary cluster enhances high-affinity IL-2 receptor expression and promotes generation of $CD8^+$ memory T cells (142, 143). A variation on this theme was shown recently by the demonstration that help to naive $CD8^+$ cells can be provided by other $CD8^+$ cells through preferential recruitment of polyclonal $CD8^+$ T cells to specific $CD8^+$ T cells responding to DCs (144). As with help delivered by $CD4^+$ T cells, the tendency for increased clustering of nonspecific polyclonal $CD8^+$ cells requires upregulation of CCR5, induced in $CD8^+$ T cells by inflammation without the need for specific antigen stimulation. Such a mechanism would encourage greater vigilance in surveying the repertoire during an ongoing immune response.

A key question is whether $CD8^+$ cells are preferentially recruited or retained (or both) by the presence of $CD4^+$ (or $CD8^+$) cells in contact with DCs. Castellino et al. (143) present evidence suggesting that $CD8^+$ cells are recruited to clusters through chemotaxis, by analyzing the hit rate of $CD8^+$ cells making contact with DC clusters. Within 25 μm of a DC, the wild-type cells show a pronounced directional bias toward the DC, and they approach clusters more frequently and with greater velocity than do CCR5-knockout cells. Although a caveat remains that guidance may involve fine DC processes (nanotubes) below the limit of optical resolution, the results of this exciting paper suggest a scenario in which preferential recruitment of $CD8^+$ cells is enabled by upregulation of the chemokine receptor CCR5 on $CD8^+$ cells following antigen stimulation in the inflammatory environment, leading to chemotaxis in response to secretion of CCL3 and CCL4 by $CD4^+$/DC clusters. By favoring prolonged contacts between $CD8^+$ T cells and DCs, the larger and longer-lasting resulting clusters would thus promote $CD8^+$ cells to express high-affinity IL-2 receptors and to become memory $CD8^+$ cells.

Dynamics of Target Cell Recognition and Lysis by Cytotoxic T Lymphocytes and NK Cells

Activated $CD8^+$ T lymphocytes and NK cells both possess the ability to recognize and kill target cells by triggered exocytosis of cytolytic granules. Two studies describe the dynamics of target cell lysis within the lymph node environment. In a beautiful, yet chilling, description of cellular genocide, Mempel and colleagues (145) imaged recognition and lysis of antigen-engaged B cells by in vivo primed $CD8^+$ cytotoxic T lymphocytes (CTL). Freshly homed and motile B cells are sampled but ignored after a short-duration encounter by CTLs when the B cell suspect lacks specific antigen. CTLs latch onto genuine B cell targets in prolonged interactions only when these surrogate targets have previously taken up the specific antigen recognized by the CTL. Then, CTL cells are taken for a ride by the B cell, with the B cells leading the way in motile conjugate pairs analagous to helper T cells interacting with activated B cells (146). Motility arrest provides the first sign of the cellular murder that is taking place. After ~10 min, the monogamous CTL/B pair stop abruptly, and 5–10 min afterward the dually labeled B cells bleed soluble CMTMR from the cytoplasm while nuclear staining remains intact. At this point, the CTL generally detaches from its victim and migrates away in search of another target. The B cell victims are observed blebbing, leaving fragments of the corpses. These cell fragments are later cleaned up by presumptive macrophages that carry fluorescent B cell body parts within granules. In a further fascinating part of this study, when antigen-specific regulatory T cells (Tregs) are present, CTLs recognize their targets and pair off in monogamous and highly motile conjugate pairs, but the targets are not killed, and the CTL/B cell conjugate pairs continue to migrate together until

the CTL eventually detach, leaving the target unscathed.

In contrast to $CD8^+$ T lymphocytes, NK cells need no initial activation and priming step to recognize and kill their target. Target recognition is not antigen specific, although in both cases the lethal hit can be delivered by exocytosis of cytolytic granules or by ligand-induced death. NK cells are restrained from killing through engagement of inhibitory receptors that recognize self–MHC class I. Failure to recognize self–MHC I in combination with activating signals unleashes the lethal potential of NK cells, and their cytotoxic granule contents are released following contact. NK cells reject metastatic cells and bone marrow transplants from MHC-mismatched donors by this mechanism. In the lymph node, NK cells actively patrol the territory near B cell follicles, migrating at 6–7 μm/min (104). Garrod et al. (104) set up allogeneic foreign B cells as potential NK cell targets along with cotransferred syngeneic B cells. Both syngeneic and allogeneic cells migrate at 5–7 μm/min, and NK cells sample both in a series of short contacts. When allogeneic MHC-mismatched B cells are recognized, NK interactions are prolonged and the B cell targets stop moving. Sometimes several NK cells swarmed a common B cell target. Shortly after dissociation of cognate NK cells, allogeneic B cell blebbing and fragmentation occurred.

Regulatory T Cells

Regulatory T cells (Tregs) modulate numerous types of immune responses and protect against autoimmunity by inhibiting activation responses during antigen priming through mechanisms that may require direct contact between Tregs and DCs and/or bystander effects mediated by cytokines (147–151). Three papers have applied immunoimaging techniques to investigate these processes in different settings of specific T cell priming by introducing Tregs as purified $CD25^+$ cell populations [Foxp3 GFP cells (151) would be an attractive alternative but unfortunately have low fluorescence].

In a model of type 1 diabetes, $CD4^+$ T (Th) cells specific for islet autoantigens are highly motile and migrate randomly in nondraining inguinal lymph node but swarm and arrest in pancreatic lymph nodes of prediabetic NOD (nonobese diabetic) animals (152). Antigen-specific Tregs behave similarly in both environments. In $CD28^{-/-}$ NOD hosts with fewer Tregs, autoimmune progression is more rapid, and the static clusters of Th cells are predominant. When cotransferred together with $CD25^+$ Tregs, little change is evident, but Tregs transferred ahead of time inhibit swarming and cluster formation of diabetogenic Th cells. Imaging both cells together shows that the presence of Tregs prevents swarming and arrest of Th cells, but without apparent direct interactions. In pancreatic lymph node, where DCs were visible because they had taken up GFP released by dying β cells, dynamic but stable contacts between Th cells and DCs, as well as swarming activity, were observed, reminiscent of T cell/DC dynamics during CD4 T cell priming (117). Tregs also swarm and engage in long-lasting interactions with DCs, but their presence inhibits stable contacts of Th cells with DCs.

These results point strongly to indirect actions of Tregs on Th cells, possibly mediated by DCs. Could it be that Tregs somehow reduce the quantity of specific antigen on DCs, or do they produce factors that inhibit antigen recognition by Th cells? Without visualizing Tregs directly, Tadokoro et al. (153) showed that the presence of Tregs inhibits stable contacts of autoreactive myelin basic protein-specific T cells with autoantigen presented in the lymph node following an immunization by injected myelin basic protein. The presence of Tregs in both systems favors robust, apparently normal motility of $CD4^+$ T cells, despite the presence of autoantigens, by inhibition of antigen recognition and the stop signal subsequent to interaction with autoantigen-presenting DCs.

A somewhat different picture of Treg action was obtained by Mempel and colleagues (145) while imaging the ability of $CD8^+$ CTLs interacting with antigen-presenting target cells. Instead of altering the initial recognition and stable attachment to an APC, Tregs do not inhibit CTL recognition and stable interactions with B cell targets. Instead, Tregs profoundly inhibit the ability of $CD8^+$ CTLs to release cytolytic granules and to lyse the targets (145). Despite being fully armed, potentially dangerous, and in contact with a target that would otherwise be destroyed, CTLs do not deliver the lethal hit. Tregs themselves were imaged in this study but did not interact directly with $CD8^+$ effectors. The ability of Tregs to suppress $CD8^+$ cytolytic function depends on TGF-β production. These results (145) indicate that Tregs can prevent the final cytolytic step of CTL-target interaction but do not interfere with all the previous steps, including initial CTL priming and their subsequent recognition and long-lasting conjugate interaction with the target. A picture thus emerges from these imaging studies that Tregs can exert effects both on initial recognition with APCs and on subsequent activation events.

Activation of B Lymphocytes

B cells exhibit great flexibility to capture and respond to antigen in varying contexts. B cells at the follicle edge acquire, sample, and respond to antigen diffusing in or held by macrophages and FDCs. B cells in the follicle interior sample FDCs for antigen captured and displayed on their surface, activate, and then migrate to the edge of the T cell area. In contrast, newly homed B cells sample, respond to, and capture whole antigen displayed on the surface of DCs in the paracortex. T cell help delivered to B cells by direct cell contact is required for B cell immunoglobulin class switching and hypermutation in germinal centers to become high-affinity antibody-producing plasma cells. Live-cell immunoimaging is now illuminating the underlying choreography of each of these events.

B cell–DC interaction. A recent paper presents a fascinating scenario for newly homed B cells on their way to the follicle to interact with cognate antigen-bearing DCs in the paracortex. When specific antigen corresponding to the BCR is present, B cell contact with DC results in B cell Ca^{2+} signaling, cell arrest, and antigen uptake by newly homed B cells. Qi et al. (113) show that B cells emerging from HEVs make contact with DCs immediately after homing. Soluble antigen, delivered through reticular conduits, is taken up by the DC and presented, in a form recognized by the BCR (i.e., without complete processing to small peptide fragments bound to MHC) to B cells on their way to the follicle. Ca^{2+} signaling is rapidly initiated, and the B cells fail to localize to the follicle but linger in direct contact with DCs while upregulating surface expression of the chemokine receptor CCR7 and CD86, the costimulatory ligand for CD28 on T cells. This hit and run robbery of antigen provides an opportunity for a localized ménage à trois, consisting of DCs, T cells, and B cells interacting together locally in the cortical ridge. Thus, DCs may provide a platform for localized T cell–B cell interaction that would potentially accelerate the delivery of T cell help to activating B cells.

B cells seeking help by chemotaxis. B cells that are already in the follicle respond to the arrival of antigen in a very different manner. In the absence of antigen, B cells migrate inside the follicle at 6–7 μm/min and follow random trajectories (2). In order for B cells to receive T cell help during antigen challenge, they must make direct contact with $CD4^+$ T cells by migrating to the edge of the follicle (follicular exclusion) after detecting the presence of antigen with their BCRs. Studies by Okada et al. (154) reveal that this is achieved by directed migration of antigen-engaged B cells, rather than by trapping of cells that randomly arrive at the follicle edge (146).

Antigen induces a rapid upregulation of CCR7 expression that may permit the cells to detect and then migrate directionally along a CCL21 gradient (visualized by immunostaining) projecting from the T cell zone ~150 μm into the follicle. Initially, antigen-engaged B cells move at a reduced rate (4 μm/min) but then later migrate more rapidly, after 1 day at 8–9 μm/min. Recent studies have confirmed the initial decline in B cell velocity upon antigen engagement, first seen by Okada et al. (146), by visualizing B cells following subcutaneous injection of antigen-coated small particles (112) or antigen-containing immune complexes (23). Okada et al. (146) then went on to show that upon reaching the CCL21 gradient by random migration, the B cells dither but then make consistent progress along more linear paths toward the T zone (a B-line, so to speak). Further supporting this interpretation, Okada et al. (154) showed that $CCR7^{-/-}$ antigen-specific B cells fail to relocate, as do $CCR7^{+/+}$ in plt recipients that lack CCL19 and CCL21, consistent with conclusions from static imaging of fixed tissue (51). The directed migration of B cells may be the first example in which chemotaxis (or more properly haptotaxis) of lymphocytes has been clearly visualized in the lymph node.

T cells delivering help: B cell/T cell waltz at the follicle edge. B cells that encounter activated T cells at the edge of the follicle form stable, motile conjugate pairs and migrate as partners, waltzing at the follicle edge with the characteristic velocity of an activated B cell (146). The B cell always leads, dragging the T cell behind as a rounded partner, sharing the dance floor with activated solitary T and B cells. Although generally stable (with contacts often lasting >45 min), conjugate pairs also undergo partner exchange, with single B or T cells cutting in on a motile pair. Activated solitary T and B cells that have not yet paired off migrate in the same region with conjugate pairs, the T cells more rapidly at ~12 μm/min. During partner exchange, contact between two Bs and one T or between one B and two Ts (threesomes) rarely lasts more than a minute or two before the new T/B pair moves away (146), resulting in serial monogamy. Rare long-lasting threesomes do not migrate effectively.

T cell help to B cells promotes differentiation of B cells to antibody-producing plasma cells. But what purpose might be served by the motility of cognate T/B pairs and by partner exchange? As B cells present antigen to T cells, the resultant T cell Ca^{2+} signaling will inhibit T cell motility, permitting coordinated motion to be led by the B cell. Polarized cytokine secretion by helper T cells in contact with B cells was discovered nearly 20 years ago (155), and more recently Huse and colleagues (137) showed that T cells can secrete certain cytokines locally toward the B cell, while releasing other cytokines and chemokines multidirectionally from the distal side of a T cell engaged with a B cell partner. Thus, polarized cytokine production in a motile conjugate pair may allow the T cell to secrete IL-2 and IFN-γ locally into the immunological synapse for a private conversation with the B cell, while at the same time broadcasting IL-4, tumor necrosis factor, and the chemokine CCL3 into the surrounding tissue. The motility of the conjugate pair would allow for more extensive distribution of inflammatory cytokines and chemokines than if the cells were immotile. Moreover, their motility may permit the conjugate pair to seek and colonize new territory, with B cells possibly carrying T cells into the follicle, and T cell/B cell partner exchange may optimize T/B cooperation during a mixed antigen response, thereby reducing the likelihood of ineffective T cell help being delivered to the B cell.

Germinal center dynamics. Germinal centers are sites of organization for B cells and FDCs, and perhaps also T cells, to interact during a developing humoral immune response. In germinal centers, the humoral immune response becomes fine-tuned to produce high-affinity antibodies generated by

hypermutation of the variable regions of the antibody locus and by selection of cells. It is thought that competition among newly arising clones underlies a survival advantage for those clones that produce the highest affinity BCR (99). Based on histological examination of fixed tissue, germinal centers are subdivided into dark zones close to the T cell region and more distal light zones. B cell blasts undergoing cell division predominate in the dark zone, and the light zone contains a network of FDCs with extensive fine processes that bind immune complexes. Three recent imaging studies have begun to examine cellular dynamics in germinal centers.

All three groups imaged highly motile B cells within the light and dark zones (21, 156, 157). B cells exhibit an elongated, dendritic morphology and migrate similarly at 6 μm/min within both regions. Two populations of B cells, including motile cells that moved along straighter paths than naive B cells and relatively stationary B cells, were distinguished in one study (21). Clusters of relatively stationary B cells make contact with FDCs, sometimes through long membrane tethers. All three groups demonstrated bidirectional migration between light and dark zones, but detailed cell tracking in favorably situated germinal centers showed surprisingly little crossing of the border between light and dark zones in two of the studies (21, 156). Furthermore, episodes of B cell division and death were seen in both light and dark zones (21). Apoptotic B cells release blebs and larger cell fragments including nuclei; both are taken up by macrophages. B cell blebs are also acquired by motile T cells that are present, mainly in the light zone and moving with higher velocity than B cells. T cells are seen to engage B cells only in short-duration contacts, suggesting limited delivery of help at this stage. One group saw frequent visits to the germinal center by follicular B cells (157); another saw B cells leaving toward the T cell area, but not toward the follicle mantle (21).

These recent imaging studies are causing reevaluation of a classical model for affinity maturation (158) to account for B cell proliferation and death in both light and dark zones and to consider the implications of a low incidence of interzonal migration (21, 99, 156). In a strict interpretation of the cyclic reentry model, somatic hypermutation during cell division in the dark zone and selection events in the light zone would require migration from the light zone to the dark zone and back to the light zone, necessitating double crossing of the zonal boundary (once in each direction) during each cell cycle. The relative infrequency of such border crossings and the corresponding primarily intrazonal pattern of migration may favor a model of intrazonal germinal center development in which B cells need not migrate to and fro in order to be selected (21). A revised cyclic reentry model would allow recombination and division in both subcompartments and considers competition for germinal center T cells to promote selection of favorable rearrangements (99). Direct tracking of antigen, along with longer-term and wider-field imaging, may help to distinguish these models or to reveal aspects of both in differing circumstances.

IMMUNOIMAGING APPLIED TO OTHER ORGANS: A BRIEF OVERVIEW

In addition to enabling the dynamics of lymphocyte motility and cellular interactions to be imaged within lymph nodes, two-photon immunoimaging is being applied in several other sites. Page constraints prohibit a detailed account of these results, but two-photon imaging has been effectively performed in spleen (159–162), thymus (1, 24, 129), bone marrow (163–165), skin (166; D. Sen, M. Matheu, M.D. Cahalan, and I. Parker, unpublished observations), gut (167, 168), the central nervous system (169, 170), and tumors (171–174). Highlights particularly relevant to themes developed in this review include the mixture of randomly oriented and highly directional paths of developing thymocytes during positive selection in the thymus (24);

gesticulation of dynamic DC dendrites into the gut lumen (168); extrusion of proto-platelets from megakaryocytes into blood vessels (165); random migration and arrest of encephalitogenic T cells invading the spinal cord and recognizing myelin autoantigens (170); and the random migration and stable target interactions of tumor-infiltrating lymphocytes (173) and cytotoxic T lymphocytes (171) in the tumor microenvironment. Random walks, chemokine receptors, antigen acquisition, cell recognition events, and stop signals no doubt apply in many of these settings.

SUMMARY AND FUTURE DIRECTIONS

The advent of two-photon microscopy allows us to visualize, in real-time and deep within intact organs and tissues, the ongoing cellular drama of the immune system under basal conditions and during responses to antigen. Although previous static imaging approaches had provided great insights, they may be likened to trying to understand the rules of baseball using only still photographs. Dynamic, multidimensional imaging is now helping us comprehend the cellular rules of the game inside the lymph node and other organs. The field has evolved beyond initial phenomenological descriptions, and quantitative analyses together with computer modeling and simulation are beginning to make sense of the apparently chaotic activity within lymph nodes as lymphocytes continually migrate amid the waving dendrites of DCs. At a macroscopic scale, random-walk motility prevails, constituting a swarm intelligence of autonomous cellular elements that enables efficient and highly sensitive scanning for rare antigens. However, at a microscopic level, the individual cell motions are clearly directed both by chemokine gradients and by structural elements, as, for example, with the antigen-induced march of the B cells toward the T cell area, the migration of $CD8^+$ cells toward DC/T cell clusters, and the regulation of lymphocyte egress from the node.

At least nine types of cellular close encounters have now been visualized by live-cell immunoimaging in the lymph node, providing fresh insight on modes of cell communication during basal migration, antigen capture, antigen recognition, cell activation, differentiation, and death. (*a*) Under basal conditions, T cells migrate along FRCs that provide haptokinetic signaling to enhance their velocity. (*b*) In their ongoing search for antigen, T cells scan dynamic DC dendrites in short-lived, randomly initiated encounters. (*c*) After emerging from the HEV into the paracortex, newly homed B cells scan the DC surface for whole antigen. (*d*) Inside the follicle, B cells migrate in direct contact with FDCs, exchanging antigen back and forth. (*e*) B cells scan subcapsular macrophages and other B cells, capture immune complexes and particulate antigen, and convey the cargo to other sites. (*f*) Upon encountering specific antigen, both T and B cells undergo Ca^{2+} signaling, arrest, and upregulation of gene expression, which lead to directed migration, cytokine secretion, and cell proliferation. (*g*) After migrating to the follicle edge, B cells pair with T cells and waltz while receiving their help. (*h*) Foreign or tumor cells are killed by activated $CD8^+$ cytolytic T cells. (*i*) Foreign cells are killed by NK cells.

The application of live-cell in vivo imaging to the immune system has just begun, and we can anticipate that technological advances in microscopy and design of improved morphological and functional probes will provide new opportunities. Purely descriptive studies are being supplanted by a new functional immunoimaging approach that takes advantage of targeted gene deletion or overexpression and the application of selective pharmacological agents or antibodies to pinpoint molecular targets. Particularly important developments will be to apply immunoimaging to visualize host/pathogen dynamics and to elucidate and refine the actions of therapeutic agents at the level of cellular dynamics. Ultimately,

these methods may be applied to diagnose and treat human disease as well as continue to illuminate cellular and molecular mechanisms in the immune response.

DISCLOSURE STATEMENT

The authors are not aware of any biases that might be perceived as affecting the objectivity of this review.

ACKNOWLEDGMENTS

The authors thank members of our joint laboratory group—Melanie Matheu, Debasish Sen, Ying Yu, and Kym Garrod—for their comments on the manuscript, and M. Matheu and Y. Yu for assistance in preparing figures. In addition, we wish to thank Mark Miller (Washington University) and David Fruman (University of California, Irvine) for their careful reading and helpful suggestions. This work is supported by grants from the National Institutes of Health (GM41514 to M.D.C. and GM-48071 to I.P.).

LITERATURE CITED

1. Bousso P, Bhakta NR, Lewis RS, Robey E. 2002. Dynamics of thymocyte-stromal cell interactions visualized by two-photon microscopy. *Science* 296:1876–80
2. Miller MJ, Wei SH, Parker I, Cahalan MD. 2002. Two-photon imaging of lymphocyte motility and antigen response in intact lymph node. *Science* 296:1869–73
3. Stoll S, Delon J, Brotz TM, Germain RN. 2002. Dynamic imaging of T cell-dendritic cell interactions in lymph nodes. *Science* 296:1873–76
4. Petty HR. 2007. Fluorescence microscopy: established and emerging methods, experimental strategies, and applications in immunology. *Microsc. Res. Tech.* 70:687–709
5. Nimmerjahn A, Kirchhoff F, Helmchen F. 2005. Resting microglial cells are highly dynamic surveillants of brain parenchyma in vivo. *Science* 308:1314–18
6. Oheim M, Beaurepaire E, Chaigneau E, Mertz J, Charpak S. 2001. Two-photon microscopy in brain tissue: parameters influencing the imaging depth. *J. Neurosci. Methods* 111:29–37
7. Cahalan MD, Parker I, Wei SH, Miller MJ. 2002. Two-photon tissue imaging: seeing the immune system in a fresh light. *Nat. Rev. Immunol.* 2:872–80
8. Germain RN, Miller MJ, Dustin ML, Nussenzweig MC. 2006. Dynamic imaging of the immune system: progress, pitfalls and promise. *Nat. Rev. Immunol.* 6:497–507
9. Mempel TR, Scimone ML, Mora JR, von Andrian UH. 2004. In vivo imaging of leukocyte trafficking in blood vessels and tissues. *Curr. Opin. Immunol.* 16:406–17
10. Dickinson ME, Simbuerger E, Zimmermann B, Waters CW, Fraser SE. 2003. Multiphoton excitation spectra in biological samples. *J. Biomed. Opt.* 8:329–38
11. Mertz J. 2004. Nonlinear microscopy: new techniques and applications. *Curr. Opin. Neurobiol.* 14:610–16
12. Mohler W, Millard AC, Campagnola PJ. 2003. Second harmonic generation imaging of endogenous structural proteins. *Methods* 29:97–109
13. Levene MJ, Dombeck DA, Kasischke KA, Molloy RP, Webb WW. 2004. In vivo multiphoton microscopy of deep brain tissue. *J. Neurophysiol.* 91:1908–12
14. Booth MJ, Neil MA, Juskaitis R, Wilson T. 2002. Adaptive aberration correction in a confocal microscope. *Proc. Natl. Acad. Sci. USA* 99:5788–92

15. Niesner RA, Andresen V, Neumann J, Spiecker H, Gunzer M. 2007. The power of single- and multibeam 2-photon microscopy for high-resolution and high-speed deep tissue and intravital imaging. *Biophys. J.* 93:2519–29
16. Gobel W, Kerr JN, Nimmerjahn A, Helmchen F. 2004. Miniaturized two-photon microscope based on a flexible coherent fiber bundle and a gradient-index lens objective. *Opt. Lett.* 29:2521–23
17. Jung JC, Mehta AD, Aksay E, Stepnoski R, Schnitzer MJ. 2004. In vivo mammalian brain imaging using one- and two-photon fluorescence microendoscopy. *J. Neurophysiol.* 92:3121–33
18. Giepmans BN, Adams SR, Ellisman MH, Tsien RY. 2006. The fluorescent toolbox for assessing protein location and function. *Science* 312:217–24
19. Straight AF. 2007. Fluorescent protein applications in microscopy. *Methods Cell Biol.* 81:93–113
20. Spiess E, Bestvater F, Heckel-Pompey A, Toth K, Hacker M, et al. 2005. Two-photon excitation and emission spectra of the green fluorescent protein variants ECFP, EGFP and EYFP. *J. Microsc.* 217:200–4
21. Hauser AE, Junt T, Mempel TR, Sneddon MW, Kleinstein SH, et al. 2007. Definition of germinal-center B cell migration in vivo reveals predominant intrazonal circulation patterns. *Immunity* 26:655–67
22. Lindquist RL, Shakhar G, Dudziak D, Wardemann H, Eisenreich T, et al. 2004. Visualizing dendritic cell networks in vivo. *Nat. Immunol.* 5:1243–50
23. Phan TG, Grigorova I, Okada T, Cyster JG. 2007. Subcapsular encounter and complement-dependent transport of immune complexes by lymph node B cells. *Nat. Immunol.* 8:992–1000
24. Witt CM, Raychaudhuri S, Schaefer B, Chakraborty AK, Robey EA. 2005. Directed migration of positively selected thymocytes visualized in real time. *PLoS Biol.* 3:1062–69
25. Bajenoff M, Egen JG, Koo LY, Laugier JP, Brau F, et al. 2006. Stromal cell networks regulate lymphocyte entry, migration, and territoriality in lymph nodes. *Immunity* 25:989–1001
26. Miller MJ, Wei SH, Cahalan MD, Parker I. 2003. Autonomous T cell trafficking examined in vivo with intravital two-photon microscopy. *Proc. Natl. Acad. Sci. USA* 100:2604–9
27. Sumen C, Mempel TR, Mazo IB, von Andrian UH. 2004. Intravital microscopy: visualizing immunity in context. *Immunity* 21:315–29
28. Gowans JL. 1959. The recirculation of lymphocytes from blood to lymph in the rat. *J. Physiol.* 146:54–69
29. Gowans JL, Knight EJ. 1964. The route of re-circulation of lymphocytes in the rat. *Proc. R. Soc. London B Biol. Sci.* 159:257–82
30. Marchesi VT, Gowans JL. 1964. The migration of lymphocytes through the endothelium of venules in lymph nodes: an electron microscope study. *Proc. R. Soc. London B Biol. Sci.* 159:283–90
31. Campbell DJ, Kim CH, Butcher EC. 2003. Chemokines in the systemic organization of immunity. *Immunol. Rev.* 195:58–71
32. Gallatin WM, Weissman IL, Butcher EC. 1983. A cell-surface molecule involved in organ-specific homing of lymphocytes. *Nature* 304:30–34
33. Gutman GA, Weissman IL. 1972. Lymphoid tissue architecture. Experimental analysis of the origin and distribution of T-cells and B-cells. *Immunology* 23:465–79
34. von Andrian UH, Mempel TR. 2003. Homing and cellular traffic in lymph nodes. *Nat. Rev. Immunol.* 3:867–78

35. de Boisfleury-Chevance A, Rapp B, Gruler H. 1989. Locomotion of white blood cells: a biophysical analysis. *Blood Cells* 15:315–33
36. Haston WS, Shields JM, Wilkinson PC. 1982. Lymphocyte locomotion and attachment on two-dimensional surfaces and in three-dimensional matrices. *J. Cell Biol.* 92:747–52
37. Noble PB, Boyarsky A, Bentley KC. 1979. Human lymphocyte migration in vitro: characterization and quantitation of locomotory parameters. *Can. J. Physiol. Pharmacol.* 57:108–12
38. Negulescu PA, Krasieva TB, Khan A, Kerschbaum HH, Cahalan MD. 1996. Polarity of T cell shape, motility, and sensitivity to antigen. *Immunity* 4:421–30
39. Groves JT, Dustin ML. 2003. Supported planar bilayers in studies on immune cell adhesion and communication. *J. Immunol. Methods* 278:19–32
40. Friedl P, den Boer AT, Gunzer M. 2005. Tuning immune responses: diversity and adaptation of the immunological synapse. *Nat. Rev. Immunol.* 5:532–45
41. Gunzer M, Schafer A, Borgmann S, Grabbe S, Zanker KS, et al. 2000. Antigen presentation in extracellular matrix: interactions of T cells with dendritic cells are dynamic, short lived, and sequential. *Immunity* 13:323–32
42. Gunzer M, Weishaupt C, Hillmer A, Basoglu Y, Friedl P, et al. 2004. A spectrum of biophysical interaction modes between T cells and different antigen-presenting cells during priming in 3-D collagen and in vivo. *Blood* 104:2801–9
43. Stachowiak AN, Wang Y, Huang YC, Irvine DJ. 2006. Homeostatic lymphoid chemokines synergize with adhesion ligands to trigger T and B lymphocyte chemokinesis. *J. Immunol.* 177:2340–48
44. Doh J, Irvine DJ. 2006. Immunological synapse arrays: patterned protein surfaces that modulate immunological synapse structure formation in T cells. *Proc. Natl. Acad. Sci. USA* 103:5700–5
45. Dustin ML, Bromley SK, Kan Z, Peterson DA, Unanue ER. 1997. Antigen receptor engagement delivers a stop signal to migrating T lymphocytes. *Proc. Natl. Acad. Sci. USA* 94:3909–13
46. Huang AY, Qi H, Germain RN. 2004. Illuminating the landscape of in vivo immunity: insights from dynamic in situ imaging of secondary lymphoid tissues. *Immunity* 21:331–39
47. Huang JH, Cardenas-Navia LI, Caldwell CC, Plumb TJ, Radu CG, et al. 2007. Requirements for T lymphocyte migration in explanted lymph nodes. *J. Immunol.* 178:7747–55
48. Worbs T, Mempel TR, Bolter J, von Andrian UH, Forster R. 2007. CCR7 ligands stimulate the intranodal motility of T lymphocytes in vivo. *J. Exp. Med.* 204:489–95
49. Mempel TR, Henrickson SE, Von Andrian UH. 2004. T-cell priming by dendritic cells in lymph nodes occurs in three distinct phases. *Nature* 427:154–59
50. Shakhar G, Lindquist RL, Skokos D, Dudziak D, Huang JH, et al. 2005. Stable T cell-dendritic cell interactions precede the development of both tolerance and immunity in vivo. *Nat. Immunol.* 6:707–14
51. Reif K, Ekland EH, Ohl L, Nakano H, Lipp M, et al. 2002. Balanced responsiveness to chemoattractants from adjacent zones determines B-cell position. *Nature* 416:94–99
52. Cyster JG. 2005. Chemokines, sphingosine-1-phosphate, and cell migration in secondary lymphoid organs. *Annu. Rev. Immunol.* 23:127–59
53. Gretz JE, Anderson AO, Shaw S. 1997. Cords, channels, corridors and conduits: critical architectural elements facilitating cell interactions in the lymph node cortex. *Immunol. Rev.* 156:11–24
54. Anderson AO, Anderson ND. 1975. Studies on the structure and permeability of the microvasculature in normal rat lymph nodes. *Am. J. Pathol.* 80:387–418

55. Gretz JE, Norbury CC, Anderson AO, Proudfoot AE, Shaw S. 2000. Lymph-borne chemokines and other low molecular weight molecules reach high endothelial venules via specialized conduits while a functional barrier limits access to the lymphocyte microenvironments in lymph node cortex. *J. Exp. Med.* 192:1425–40
56. Katakai T, Hara T, Lee JH, Gonda H, Sugai M, Shimizu A. 2004. A novel reticular stromal structure in lymph node cortex: an immuno-platform for interactions among dendritic cells, T cells and B cells. *Int. Immunol.* 16:1133–42
57. Asperti-Boursin F, Real E, Bismuth G, Trautmann A, Donnadieu E. 2007. CCR7 ligands control basal T cell motility within lymph node slices in a phosphoinositide 3-kinase-independent manner. *J. Exp. Med.* 204:1167–79
58. Friedman RS, Jacobelli J, Krummel MF. 2006. Surface-bound chemokines capture and prime T cells for synapse formation. *Nat. Immunol.* 7:1101–8
59. Weninger W, von Andrian UH. 2003. Chemokine regulation of naive T cell traffic in health and disease. *Semin. Immunol.* 15:257–70
60. Zlotnik A, Yoshie O, Nomiyama H. 2006. The chemokine and chemokine receptor superfamilies and their molecular evolution. *Genome Biol.* 7:243
61. Viola A, Contento RL, Molon B. 2006. T cells and their partners: the chemokine dating agency. *Trends Immunol.* 27:421–27
62. Rot A, von Andrian UH. 2004. Chemokines in innate and adaptive host defense: basic chemokinese grammar for immune cells. *Annu. Rev. Immunol.* 22:891–928
63. Woolf E, Grigorova I, Sagiv A, Grabovsky V, Feigelson SW, et al. 2007. Lymph node chemokines promote sustained T lymphocyte motility without triggering stable integrin adhesiveness in the absence of shear forces. *Nat. Immunol.* 8:1076–85
64. Okada T, Cyster JG. 2007. CC chemokine receptor 7 contributes to Gi-dependent T cell motility in the lymph node. *J. Immunol.* 178:2973–78
65. Han SB, Moratz C, Huang NN, Kelsall B, Cho H, et al. 2005. Rgs1 and Gnai2 regulate the entrance of B lymphocytes into lymph nodes and B cell motility within lymph node follicles. *Immunity* 22:343–54
66. Hwang IY, Park C, Kehrl JH. 2007. Impaired trafficking of *Gnai2*$^{+/-}$ and *Gnai2*$^{-/-}$ T lymphocytes: implications for T cell movement within lymph nodes. *J. Immunol.* 179:439–48
67. Luther SA, Bidgol A, Hargreaves DC, Schmidt A, Xu Y, et al. 2002. Differing activities of homeostatic chemokines CCL19, CCL21, and CXCL12 in lymphocyte and dendritic cell recruitment and lymphoid neogenesis. *J. Immunol.* 169:424–33
68. Hogg N, Smith A, McDowall A, Giles K, Stanley P, et al. 2004. How T cells use LFA-1 to attach and migrate. *Immunol. Lett.* 92:51–54
69. Merlot S, Firtel RA. 2003. Leading the way: directional sensing through phosphatidylinositol 3-kinase and other signaling pathways. *J. Cell Sci.* 116:3471–78
70. Matheu MP, Deane JA, Parker I, Fruman DA, Cahalan MD. 2007. Class IA phosphoinositide 3-kinase modulates basal lymphocyte motility in the lymph node. *J. Immunol.* 179:2261–69
71. Reif K, Okkenhaug K, Sasaki T, Penninger JM, Vanhaesebroeck B, Cyster JG. 2004. Cutting edge: differential roles for phosphoinositide 3-kinases, p110γ and p110δ, in lymphocyte chemotaxis and homing. *J. Immunol.* 173:2236–40
72. Nombela-Arrieta C, Lacalle RA, Montoya MC, Kunisaki Y, Megias D, et al. 2004. Differential requirements for DOCK2 and phosphoinositide-3-kinase γ during T and B lymphocyte homing. *Immunity* 21:429–41
73. Hirsch E, Katanaev VL, Garlanda C, Azzolino O, Pirola L, et al. 2000. Central role for G protein-coupled phosphoinositide 3-kinase γ in inflammation. *Science* 287:1049–53

74. Li Z, Jiang H, Xie W, Zhang Z, Smrcka AV, Wu D. 2000. Roles of PLC-β2 and -β3 and PI3Kγ in chemoattractant-mediated signal transduction. *Science* 287:1046–49
75. Sasaki T, Irie-Sasaki J, Jones RG, Oliveira-dos-Santos AJ, Stanford WL, et al. 2000. Function of PI3Kγ in thymocyte development, T cell activation, and neutrophil migration. *Science* 287:1040–46
76. Nombela-Arrieta C, Mempel TR, Soriano SF, Mazo I, Wymann MP, et al. 2007. A central role for DOCK2 during interstitial lymphocyte motility and sphingosine-1-phosphate-mediated egress. *J. Exp. Med.* 204:497–510
77. Shulman Z, Pasvolsky R, Woolf E, Grabovsky V, Feigelson SW, et al. 2006. DOCK2 regulates chemokine-triggered lateral lymphocyte motility but not transendothelial migration. *Blood* 108:2150–58
78. Fukui Y, Hashimoto O, Sanui T, Oono T, Koga H, et al. 2001. Haematopoietic cell-specific CDM family protein DOCK2 is essential for lymphocyte migration. *Nature* 412:826–31
79. Wei SH, Safrina O, Yu Y, Garrod KR, Cahalan MD, Parker I. 2007. Ca^{2+} signals in $CD4^+$ T cells during early contacts with antigen-bearing dendritic cells in lymph node. *J. Immunol.* 179:1586–94
80. Revy P, Sospedra M, Barbour B, Trautmann A. 2001. Functional antigen-independent synapses formed between T cells and dendritic cells. *Nat. Immunol.* 2:925–31
81. Delon J, Stoll S, Germain RN. 2002. Imaging of T-cell interactions with antigen presenting cells in culture and in intact lymphoid tissue. *Immunol. Rev.* 189:51–63
82. Fischer UB, Jacovetty EL, Medeiros RB, Goudy BD, Zell T, et al. 2007. MHC class II deprivation impairs CD4 T cell motility and responsiveness to antigen-bearing dendritic cells in vivo. *Proc. Natl. Acad. Sci. USA* 104:7181–86
83. Wei SH, Parker I, Miller MJ, Cahalan MD. 2003. A stochastic view of lymphocyte motility and trafficking within the lymph node. *Immunol. Rev.* 195:136–59
84. Wei SH, Rosen H, Matheu MP, Sanna MG, Wang SK, et al. 2005. Sphingosine 1-phosphate type 1 receptor agonism inhibits transendothelial migration of medullary T cells to lymphatic sinuses. *Nat. Immunol.* 6:1228–35
85. Hargreaves DC, Hyman PL, Lu TT, Ngo VN, Bidgol A, et al. 2001. A coordinated change in chemokine responsiveness guides plasma cell movements. *J. Exp. Med.* 194:45–56
86. Mandala S, Hajdu R, Bergstrom J, Quackenbush E, Xie J, et al. 2002. Alteration of lymphocyte trafficking by sphingosine-1-phosphate receptor agonists. *Science* 296:346–49
87. Sanna MG, Liao J, Jo E, Alfonso C, Ahn MY, et al. 2004. Sphingosine 1-phosphate (S1P) receptor subtypes S1P1 and S1P3, respectively, regulate lymphocyte recirculation and heart rate. *J. Biol. Chem.* 279:13839–48
88. Matloubian M, Lo CG, Cinamon G, Lesneski MJ, Xu Y, et al. 2004. Lymphocyte egress from thymus and peripheral lymphoid organs is dependent on S1P receptor 1. *Nature* 427:355–60
89. Rosen H, Goetzl EJ. 2005. Sphingosine 1-phosphate and its receptors: an autocrine and paracrine network. *Nat. Rev. Immunol.* 5:560–70
90. Rosen H, Sanna MG, Cahalan SM, Gonzalez-Cabrera PJ. 2007. Tipping the gatekeeper: S1P regulation of endothelial barrier function. *Trends Immunol.* 28:102–7
91. Sanna MG, Wang SK, Gonzalez-Cabrera PJ, Don A, Marsolais D, et al. 2006. Enhancement of capillary leakage and restoration of lymphocyte egress by a chiral $S1P_1$ antagonist in vivo. *Nat. Chem. Biol.* 2:434–41

92. Gonzalez-Cabrera PJ, Hla T, Rosen H. 2007. Mapping pathways downstream of sphingosine 1-phosphate subtype 1 by differential chemical perturbation and proteomics. *J. Biol. Chem.* 282:7254–64
93. Halin C, Scimone ML, Bonasio R, Gauguet JM, Mempel TR, et al. 2005. The S1P-analog FTY720 differentially modulates T-cell homing via HEV: T-cell-expressed S1P1 amplifies integrin activation in peripheral lymph nodes but not in Peyer patches. *Blood* 106:1314–22
94. Mempel TR, Junt T, von Andrian UH. 2006. Rulers over randomness: stroma cells guide lymphocyte migration in lymph nodes. *Immunity* 25:867–69
95. Westermann J, Bode U, Sahle A, Speck U, Karin N, et al. 2005. Naive, effector, and memory T lymphocytes efficiently scan dendritic cells in vivo: contact frequency in T cell zones of secondary lymphoid organs does not depend on LFA-1 expression and facilitates survival of effector T cells. *J. Immunol.* 174:2517–24
96. Miller MJ, Hejazi AS, Wei SH, Cahalan MD, Parker I. 2004. T cell repertoire scanning is promoted by dynamic dendritic cell behavior and random T cell motility in the lymph node. *Proc. Natl. Acad. Sci. USA* 101:998–1003
97. Cyster JG, Ansel KM, Reif K, Ekland EH, Hyman PL, et al. 2000. Follicular stromal cells and lymphocyte homing to follicles. *Immunol. Rev.* 176:181–93
98. Kosco-Vilbois MH. 2003. Are follicular dendritic cells really good for nothing? *Nat. Rev. Immunol.* 3:764–69
99. Allen CD, Okada T, Cyster JG. 2007. Germinal-center organization and cellular dynamics. *Immunity* 27:190–202
100. Moretta A, Marcenaro E, Parolini S, Ferlazzo G, Moretta L. 2007. NK cells at the interface between innate and adaptive immunity. *Cell Death Differ*. In press
101. Chen S, Kawashima H, Lowe JB, Lanier LL, Fukuda M. 2005. Suppression of tumor formation in lymph nodes by L-selectin-mediated natural killer cell recruitment. *J. Exp. Med.* 202:1679–89
102. Martin-Fontecha A, Thomsen LL, Brett S, Gerard C, Lipp M, et al. 2004. Induced recruitment of NK cells to lymph nodes provides IFN-γ for T(H)1 priming. *Nat. Immunol.* 5:1260–65
103. Bajenoff M, Breart B, Huang AY, Qi H, Cazareth J, et al. 2006. Natural killer cell behavior in lymph nodes revealed by static and real-time imaging. *J. Exp. Med.* 203:619–31
104. Garrod KR, Wei SH, Parker I, Cahalan MD. 2007. Natural killer cells actively patrol peripheral lymph nodes forming stable conjugates to eliminate MHC-mismatched targets. *Proc. Natl. Acad. Sci. USA* 104:12081–86
105. Itano AA, McSorley SJ, Reinhardt RL, Ehst BD, Ingulli E, et al. 2003. Distinct dendritic cell populations sequentially present antigen to CD4 T cells and stimulate different aspects of cell-mediated immunity. *Immunity* 19:47–57
106. Sixt M, Kanazawa N, Selg M, Samson T, Roos G, et al. 2005. The conduit system transports soluble antigens from the afferent lymph to resident dendritic cells in the T cell area of the lymph node. *Immunity* 22:19–29
107. Kissenpfennig A, Henri S, Dubois B, Laplace-Builhe C, Perrin P, et al. 2005. Dynamics and function of Langerhans cells in vivo dermal dendritic cells colonize lymph node areas distinct from slower migrating Langerhans cells. *Immunity* 22:643–54
108. MartIn-Fontecha A, Sebastiani S, Hopken UE, Uguccioni M, Lipp M, et al. 2003. Regulation of dendritic cell migration to the draining lymph node: impact on T lymphocyte traffic and priming. *J. Exp. Med.* 198:615–21

109. Agrawal S, Agrawal A, Doughty B, Gerwitz A, Blenis J, et al. 2003. Cutting edge: different Toll-like receptor agonists instruct dendritic cells to induce distinct Th responses via differential modulation of extracellular signal-regulated kinase-mitogen-activated protein kinase and c-Fos. *J. Immunol.* 171:4984–89
110. Pulendran B. 2004. Modulating vaccine responses with dendritic cells and Toll-like receptors. *Immunol. Rev.* 199:227–50
111. Pape KA, Catron DM, Itano AA, Jenkins MK. 2007. The humoral immune response is initiated in lymph nodes by B cells that acquire soluble antigen directly in the follicles. *Immunity* 26:491–502
112. Carrasco YR, Batista FD. 2007. B cells acquire particulate antigen in a macrophage-rich area at the boundary between the follicle and the subcapsular sinus of the lymph node. *Immunity* 27:160–71
113. Qi H, Egen JG, Huang AY, Germain RN. 2006. Extrafollicular activation of lymph node B cells by antigen-bearing dendritic cells. *Science* 312:1672–76
114. Bousso P, Robey E. 2003. Dynamics of $CD8^+$ T cell priming by dendritic cells in intact lymph nodes. *Nat. Immunol.* 4:579–85
115. Wei X, Tromberg BJ, Cahalan MD. 1999. Mapping the sensitivity of T cells with an optical trap: polarity and minimal number of receptors for Ca^{2+} signaling. *Proc. Natl. Acad. Sci. USA* 96:8471–76
116. Kaiser A, Donnadieu E, Abastado JP, Trautmann A, Nardin A. 2005. CC chemokine ligand 19 secreted by mature dendritic cells increases naive T cell scanning behavior and their response to rare cognate antigen. *J. Immunol.* 175:2349–56
117. Miller MJ, Safrina O, Parker I, Cahalan MD. 2004. Imaging the single cell dynamics of $CD4^+$ T cell activation by dendritic cells in lymph nodes. *J. Exp. Med.* 200:847–56
118. Feske S. 2007. Calcium signalling in lymphocyte activation and disease. *Nat. Rev. Immunol.* 7:690–702
119. Cahalan MD, Zhang SL, Yeromin AV, Ohlsen K, Roos J, Stauderman KA. 2007. Molecular basis of the CRAC channel. *Cell Calcium* 42:133–44
120. Lewis RS. 2007. The molecular choreography of a store-operated calcium channel. *Nature* 446:284–87
121. Fanger CM, Hoth M, Crabtree GR, Lewis RS. 1995. Characterization of T cell mutants with defects in capacitative calcium entry: genetic evidence for the physiological roles of CRAC channels. *J. Cell Biol.* 131:655–67
122. Feske S, Giltnane J, Dolmetsch R, Staudt LM, Rao A. 2001. Gene regulation mediated by calcium signals in T lymphocytes. *Nat. Immunol.* 2:316–24
123. Negulescu PA, Shastri N, Cahalan MD. 1994. Intracellular calcium dependence of gene expression in single T lymphocytes. *Proc. Natl. Acad. Sci. USA* 91:2873–77
124. Dolmetsch RE, Lewis RS, Goodnow CC, Healy JI. 1997. Differential activation of transcription factors induced by Ca^{2+} response amplitude and duration. *Nature* 386:855–58
125. Dolmetsch RE, Xu K, Lewis RS. 1998. Calcium oscillations increase the efficiency and specificity of gene expression. *Nature* 392:933–36
126. Skokos D, Shakhar G, Varma R, Waite JC, Cameron TO, et al. 2007. Peptide-MHC potency governs dynamic interactions between T cells and dendritic cells in lymph nodes. *Nat. Immunol.* 8:835–44
127. Donnadieu E, Cefai D, Tan YP, Paresys G, Bismuth G, Trautmann A. 1992. Imaging early steps of human T cell activation by antigen-presenting cells. *J. Immunol.* 148:2643–53
128. Donnadieu E, Bismuth G, Trautmann A. 1994. Antigen recognition by helper T cells elicits a sequence of distinct changes of their shape and intracellular calcium. *Curr. Biol.* 4:584–95

129. Bhakta NR, Oh DY, Lewis RS. 2005. Calcium oscillations regulate thymocyte motility during positive selection in the three-dimensional thymic environment. *Nat. Immunol.* 6:143–51
130. Schneider H, Downey J, Smith A, Zinselmeyer BH, Rush C, et al. 2006. Reversal of the TCR stop signal by CTLA-4. *Science* 313:1972–75
131. Cahalan MD, Gutman GA. 2006. The sense of place in the immune system. *Nat. Immunol.* 7:329–32
132. Obst R, van Santen HM, Mathis D, Benoist C. 2005. Antigen persistence is required throughout the expansion phase of a $CD4^+$ T cell response. *J. Exp. Med.* 201:1555–65
133. Kedl RM, Schaefer BC, Kappler JW, Marrack P. 2002. T cells down-modulate peptide-MHC complexes on APCs in vivo. *Nat. Immunol.* 3:27–32
134. Hugues S, Fetler L, Bonifaz L, Helft J, Amblard F, Amigorena S. 2004. Distinct T cell dynamics in lymph nodes during the induction of tolerance and immunity. *Nat. Immunol.* 5:1235–42
135. Zinselmeyer BH, Dempster J, Gurney AM, Wokosin D, Miller M, et al. 2005. In situ characterization of $CD4^+$ T cell behavior in mucosal and systemic lymphoid tissues during the induction of oral priming and tolerance. *J. Exp. Med.* 201:1815–23
136. Celli S, Garcia Z, Bousso P. 2005. CD4 T cells integrate signals delivered during successive DC encounters in vivo. *J. Exp. Med.* 202:1271–78
137. Huse M, Lillemeier BF, Kuhns MS, Chen DS, Davis MM. 2006. T cells use two directionally distinct pathways for cytokine secretion. *Nat. Immunol.* 7:247–55
138. Catron DM, Rusch LK, Hataye J, Itano AA, Jenkins MK. 2006. $CD4^+$ T cells that enter the draining lymph nodes after antigen injection participate in the primary response and become central-memory cells. *J. Exp. Med.* 203:1045–54
139. Garcia Z, Pradelli E, Celli S, Beuneu H, Simon A, Bousso P. 2007. Competition for antigen determines the stability of T cell-dendritic cell interactions during clonal expansion. *Proc. Natl. Acad. Sci. USA* 104:4553–58
140. Guarda G, Hons M, Soriano SF, Huang AY, Polley R, et al. 2007. L-selectin-negative CCR7-effector and memory $CD8^+$ T cells enter reactive lymph nodes and kill dendritic cells. *Nat. Immunol.* 8:743–52
141. Bevan MJ. 2004. Helping the $CD8^+$ T-cell response. *Nat. Rev. Immunol.* 4:595–602
142. Beuneu H, Garcia Z, Bousso P. 2006. Cutting edge: cognate CD4 help promotes recruitment of antigen-specific CD8 T cells around dendritic cells. *J. Immunol.* 177:1406–10
143. Castellino F, Germain RN. 2007. Chemokine-guided $CD4^+$ T cell help enhances generation of IL-6Rα^{high}IL-7Rα^{high} prememory $CD8^+$ T cells. *J. Immunol.* 178:778–87
144. Hugues S, Scholer A, Boissonnas A, Nussbaum A, Combadiere C, et al. 2007. Dynamic imaging of chemokine-dependent $CD8^+$ T cell help for $CD8^+$ T cell responses. *Nat. Immunol.* 8:921–30
145. Mempel TR, Pittet MJ, Khazaie K, Weninger W, Weissleder R, et al. 2006. Regulatory T cells reversibly suppress cytotoxic T cell function independent of effector differentiation. *Immunity* 25:129–41
146. Okada T, Miller MJ, Parker I, Krummel MF, Neighbors M, et al. 2005. Antigen-engaged B cells undergo chemotaxis toward the T zone and form motile conjugates with helper T cells. *PLoS Biol.* 3:1047–61
147. Fontenot JD, Rudensky AY. 2005. A well adapted regulatory contrivance: regulatory T cell development and the forkhead family transcription factor Foxp3. *Nat. Immunol.* 6:331–37

148. Sakaguchi S, Sakaguchi N, Asano M, Itoh M, Toda M. 1995. Immunologic self-tolerance maintained by activated T cells expressing IL-2 receptor α-chains (CD25). Breakdown of a single mechanism of self-tolerance causes various autoimmune diseases. *J. Immunol.* 155:1151–64
149. Shevach EM. 2000. Regulatory T cells in autoimmmunity. *Annu. Rev. Immunol.* 18:423–49
150. von Boehmer H. 2005. Mechanisms of suppression by suppressor T cells. *Nat. Immunol.* 6:338–44
151. Fontenot JD, Rasmussen JP, Williams LM, Dooley JL, Farr AG, Rudensky AY. 2005. Regulatory T cell lineage specification by the forkhead transcription factor Foxp3. *Immunity* 22:329–41
152. Tang Q, Adams JY, Tooley AJ, Bi M, Fife BT, et al. 2006. Visualizing regulatory T cell control of autoimmune responses in nonobese diabetic mice. *Nat. Immunol.* 7:83–92
153. Tadokoro CE, Shakhar G, Shen S, Ding Y, Lino AC, et al. 2006. Regulatory T cells inhibit stable contacts between $CD4^+$ T cells and dendritic cells in vivo. *J. Exp. Med.* 203:505–11
154. Okada T, Cyster JG. 2006. B cell migration and interactions in the early phase of antibody responses. *Curr. Opin. Immunol.* 18:278–85
155. Poo WJ, Conrad L, Janeway CA Jr. 1988. Receptor-directed focusing of lymphokine release by helper T cells. *Nature* 332:378–80
156. Allen CD, Okada T, Tang HL, Cyster JG. 2007. Imaging of germinal center selection events during affinity maturation. *Science* 315:528–31
157. Schwickert TA, Lindquist RL, Shakhar G, Livshits G, Skokos D, et al. 2007. In vivo imaging of germinal centres reveals a dynamic open structure. *Nature* 446:83–87
158. MacLennan IC. 1994. Germinal centers. *Annu. Rev. Immunol.* 12:117–39
159. Grayson MH, Hotchkiss RS, Karl IE, Holtzman MJ, Chaplin DD. 2003. Intravital microscopy comparing T lymphocyte trafficking to the spleen and the mesenteric lymph node. *Am. J. Physiol. Heart Circ. Physiol.* 284:H2213–26
160. Morelli AE, Larregina AT, Shufesky WJ, Zahorchak AF, Logar AJ, et al. 2003. Internalization of circulating apoptotic cells by splenic marginal zone dendritic cells: dependence on complement receptors and effect on cytokine production. *Blood* 101:611–20
161. Odoardi F, Kawakami N, Li Z, Cordiglieri C, Streyl K, et al. 2007. Instant effect of soluble antigen on effector T cells in peripheral immune organs during immunotherapy of autoimmune encephalomyelitis. *Proc. Natl. Acad. Sci. USA* 104:920–25
162. Wei SH, Miller MJ, Cahalan MD, Parker I. 2002. Two-photon imaging in intact lymphoid tissue. *Adv. Exp. Med. Biol.* 512:203–8
163. Cavanagh LL, Bonasio R, Mazo IB, Halin C, Cheng G, et al. 2005. Activation of bone marrow-resident memory T cells by circulating, antigen-bearing dendritic cells. *Nat. Immunol.* 6:1029–37
164. Cariappa A, Mazo IB, Chase C, Shi HN, Liu H, et al. 2005. Perisinusoidal B cells in the bone marrow participate in T-independent responses to blood-borne microbes. *Immunity* 23:397–407
165. Junt T, Schulze H, Chen Z, Massberg S, Goerge T, et al. 2007. Dynamic visualization of thrombopoiesis within bone marrow. *Science* 317:1767–70
166. Chakraverty R, Cote D, Buchli J, Cotter P, Hsu R, et al. 2006. An inflammatory checkpoint regulates recruitment of graft-versus-host reactive T cells to peripheral tissues. *J. Exp. Med.* 203:2021–31

167. Tutsch E, Griesemer D, Schwarz A, Stallmach A, Hoth M. 2004. Two-photon analysis of calcium signals in T lymphocytes of intact lamina propria from human intestine. *Eur. J. Immunol.* 34:3477–84
168. Chieppa M, Rescigno M, Huang AY, Germain RN. 2006. Dynamic imaging of dendritic cell extension into the small bowel lumen in response to epithelial cell TLR engagement. *J. Exp. Med.* 203:2841–52
169. Nitsch R, Pohl EE, Smorodchenko A, Infante-Duarte C, Aktas O, Zipp F. 2004. Direct impact of T cells on neurons revealed by two-photon microscopy in living brain tissue. *J. Neurosci.* 24:2458–64
170. Kawakami N, Nagerl UV, Odoardi F, Bonhoeffer T, Wekerle H, Flugel A. 2005. Live imaging of effector cell trafficking and autoantigen recognition within the unfolding autoimmune encephalomyelitis lesion. *J. Exp. Med.* 201:1805–14
171. Boissonnas A, Fetler L, Zeelenberg IS, Hugues S, Amigorena S. 2007. In vivo imaging of cytotoxic T cell infiltration and elimination of a solid tumor. *J. Exp. Med.* 204:345–56
172. Wolf K, Mazo I, Leung H, Engelke K, von Andrian UH, et al. 2003. Compensation mechanism in tumor cell migration: mesenchymal-amoeboid transition after blocking of pericellular proteolysis. *J. Cell Biol.* 160:267–77
173. Mrass P, Takano H, Ng LG, Daxini S, Lasaro MO, et al. 2006. Random migration precedes stable target cell interactions of tumor-infiltrating T cells. *J. Exp. Med.* 203:2749–61
174. Skala MC, Squirrell JM, Vrotsos KM, Eickhoff JC, Gendron-Fitzpatrick A, et al. 2005. Multiphoton microscopy of endogenous fluorescence differentiates normal, precancerous, and cancerous squamous epithelial tissues. *Cancer Res.* 65:1180–86